

The dud canard: Existence of strong canard cycles in \mathbb{R}^3

Kristiansen, K. U.

Department of Applied Mathematics and Computer Science,
 Technical University of Denmark,
 2800 Kgs. Lyngby,
 Denmark,
 krkri@dtu.dk

July 5, 2022

Abstract

In this paper, we provide a rigorous description of the birth of canard limit cycles in slow-fast systems in \mathbb{R}^3 through the folded saddle-node of type II and the singular Hopf bifurcation. In particular, we prove – in the analytic case only – that for all $0 < \epsilon \ll 1$ there is a locally unique family of periodic orbits, born in the (singular) Hopf bifurcation and extending to $\mathcal{O}(1)$ cycles that follow the strong canard of the folded saddle-node. Our results can be seen as an extension of the canard explosion in \mathbb{R}^2 , but in contrast to the planar case, the family of periodic orbits in \mathbb{R}^3 is not explosive. For this reason, we have chosen to call the phenomena in \mathbb{R}^3 , the “dud canard”. The main difficulty of the proof lies in connecting the Hopf cycles with the canard cycles, since these are described in different scalings. As in \mathbb{R}^2 we use blowup to overcome this, but we also have to compensate for the lack of uniformity near the Hopf, due to its singular nature. We do this, by imposing analyticity of the vector-field. This allows us to prove existence of an invariant slow manifold, that is not normally hyperbolic.

Contents

1	Introduction	2
1.1	Setting	4
1.2	Main result	5
1.3	Overview	7
2	Existence of small periodic orbits	7
2.1	Existence of an analytic slow manifold	9
2.2	Melnikov theory	12
3	Existence of intermediate periodic orbits	15
3.1	Analysis in the $\bar{x} = -1$ -chart	16
3.2	Analysis in the $\bar{\epsilon} = 1$ -chart	22
3.3	Putting it all together	23
4	Completing the proof of Theorem 1.1	27
5	Discussion	28

1 Introduction

In this paper, we consider slow-fast systems of the form

$$\begin{aligned}\dot{u} &= \epsilon U(u, v, \epsilon), \\ \dot{v} &= V(u, v, \epsilon),\end{aligned}\tag{1}$$

with U and V sufficiently smooth and $0 < \epsilon \ll 1$. Systems of this form occur in many different applications, including neuroscience [1, 25, 38], biology and chemical reaction networks [16, 20] and many other areas, see [13, 35] for further references. Geometric Singular Perturbation Theory [26] is a collection of methods, based upon the ground-breaking work of Fenichel [17, 18, 19], that can be used to study systems of the form (1) for $0 < \epsilon \ll 1$. The point of departure for this theory, is the critical manifold

$$S = \{(u, v) | V(u, v, 0) = 0\},$$

which is a set of equilibria for the associated layer problem:

$$\begin{aligned}\dot{u} &= 0, \\ \dot{v} &= V(u, v, 0),\end{aligned}\tag{2}$$

obtained by setting $\epsilon = 0$ in (1). S is said to be normally hyperbolic if all eigenvalues of $D_v V(u, v)$ for all $(u, v) \in S$ have nonzero real part. In particular, it is attracting (repelling) if the real part of these eigenvalues is negative (positive, respectively). Fenichel's theory, see [17, 18, 19, 26], then says that compact submanifolds S_0 of S perturb to diffeomorphic locally invariant manifolds S_ϵ for all $0 < \epsilon \ll 1$. The reduced flow on S_ϵ is to leading order given by the reduced problem:

$$\begin{aligned}u' &= U(u, v, 0), \\ 0 &= V(u, v, 0),\end{aligned}$$

obtained by writing (1) in terms of the slow time $\tau = t\epsilon^{-1}$ with $(\prime) = \frac{d}{d\tau}$ and subsequently letting $\epsilon \rightarrow 0$. Moreover, stable and unstable manifolds of S_0 also perturb to $W^s(S_\epsilon)$ and $W^u(S_\epsilon)$, each having invariant foliations by fibers; for full details see e.g. [26].

Following work by Dumortier and Roussarie on the blowup method [15], there was in the early parts of the 2000s an effort [32, 33, 34, 39, 43] to extend the geometric theory of Fenichel to points where normal hyperbolicity breaks down. The simplest type of breakdown is perhaps observed in \mathbb{R}^2 and \mathbb{R}^3 with S having folds, that divide the critical manifold into attracting and repelling subsets. In these cases, canard solutions are solutions of (1) for $0 < \epsilon \ll 1$ that – counter-intuitively – follow the attracting and repelling branches of the critical manifold by passing close to the fold. Canards are well described in \mathbb{R}^2 and \mathbb{R}^3 [15, 6, 5, 33, 39, 34, 42] and play an important role in applications and in the global dynamics of systems of the form (1), see e.g. [13, 37, 41].

In \mathbb{R}^2 , canards of folded critical manifolds require an unfolding parameter [33] and here canard orbits may be limit cycles. In fact, the reference [33] proves that there is a family of periodic orbits – under some non-degeneracy conditions – that include small (i.e. of size $o(1)$) Hopf cycles and canard cycles of size $\mathcal{O}(1)$. Under some additional global properties, such family may be extended further to include canards with “head”, see [33], and eventually

relaxation oscillations, as in the van der Pol system [40, 33]. This situation is also known as the canard explosion [9], due to the fact that the canard limit cycles of different amplitude differ in parameter values by an order of $\mathcal{O}(e^{-c/\epsilon})$ for all $0 < \epsilon \ll 1$, see full details in [33].

In \mathbb{R}^3 , on the other hand, with $u \in \mathbb{R}^2$ and $v \in \mathbb{R}$ in (1), canards of folded critical manifolds are generic, without parameters. They appear persistently at so-called folded singularities, which are singular points on the fold of a “desingularized” reduced problem, see [5, 39]. The folded singularities come in different generic versions: folded node, folded saddle and folded focus depending on the type of singularity, with only the former two producing canard solutions.

The folded node is of particular interest due to its connection to mixed-mode oscillations. In summary, the folded node gives rise to a weak canard (under a nonresonance condition) and a strong canard – essentially due to the weak and the strong directions of the linearization of the node – and close to folded singularity, it has been shown, using blowup [39], that the tangent space of the attracting slow manifold twists a finite number of times along the weak canard. This implies, due to the contractivity towards the weak canard on the attracting side of the critical manifold, that an open set of points twist upon passage through the folded node. Upon composition with a global return mapping, this provides a simple mechanism for producing attracting limit cycles, see [10], that are of mixed-mode type, see also [13].

The folded saddle-node is a bifurcation of the folded singularity. It comes in different types I and II, but the unfolding of type II – at the level of the reduced problem – produces to a transcritical bifurcation of a true singularity and a folded one. In this paper, we will only focus on the type II and we will therefore continue to refer to this case simply as the folded saddle-node. This bifurcation is known to give rise to a Hopf bifurcation [34]. It has been called a singular Hopf bifurcation [21] due to the fact that the linearization (upon blowup) has eigenvalues of the form $\sim \pm i\omega, \sim \epsilon\lambda$, $\omega, \lambda \neq 0$ as $\epsilon \rightarrow 0$ at the Hopf; it is therefore a zero-Hopf bifurcation [3, 2] for $\epsilon = 0$.

The interest in the folded saddle-node comes from the fact that it marks the onset/termination of mixed-mode oscillations through the folded node. However, in the author’s opinion, the details of this onset/termination and the connection of mixed-mode oscillations with the Hopf cycles is still not fully understood. [10, Theorem 4.2] relates to the connection problem, but only indirectly. Specifically, the bifurcation described in this theorem – where a return mechanism transverses to the strong canard – does not relate to the Hopf bifurcation. The reference [37] is another interesting study, based upon detailed numerical computations. Here the Hopf cycles are continued using the software package AUTO and it is demonstrated (for a fixed small value of $\epsilon > 0$) that these cycles are of relaxation type without mixed-modes. In particular, the periodic orbits of mixed-mode type in the model system of [37] form isolas that are disconnected from the branch of Hopf cycles. At the same time, [21] studies a normal form for the folded saddle-node, computing the Lyapunov coefficient and demonstrating additional bifurcations (periodic doubling and torus) using numerical computations along the branch of period orbits that appear from the Hopf. [30] describes the onset of mixed-modes in a cusped saddle-node in a system with symmetry.

It has also been speculated, following work on the Koper model [28, 29], that the folded saddle-node may be associated with homoclinics and Shilnikov bifurcations. This was demonstrated for the Koper model in [23] using sophisticated numerical methods, among other things. At the same time, it is by now known [2, 8] that generic unfoldings of the zero-Hopf bifurcation produce Shilnikov bifurcations. In future work, the present author hopes to pursue these bifurcations rigorously in the context of the folded saddle-node. In preparation, we will in this paper extend the results of [33] on the family of periodic canard orbits in \mathbb{R}^2 to the \mathbb{R}^3 -context. Whereas the family of canard cycles have “explosive growth” in the

planar context, the growth rate is regular in \mathbb{R}^3 , with canard cycles of different amplitude corresponding (in general) to parameter values that differ by an $\mathcal{O}(1)$ -amount. For this reason, we have chosen to call the phenomena we describe as the “dud canard” instead of the canard explosion.

1.1 Setting

We consider the following normal form for the folded node/folded saddle-node[34]:

$$\begin{aligned} \dot{x} &= \epsilon(y - (\mu + 1)z + F(x, y, z, \epsilon, \mu)), \\ \dot{y} &= \epsilon\left(\frac{1}{2}\mu + G(x, y, z, \epsilon, \mu)\right), \\ \dot{z} &= x + z^2 + zH(x, y, z, \epsilon, \mu), \end{aligned} \tag{3}$$

in the regime $\epsilon > 0$, $\epsilon \sim 0$ and $\mu \sim 0$, where F , G and H are higher order in the following sense:

$$F(x, y, z, \epsilon, \mu) = \mathcal{O}(x, \epsilon, (|y| + |z|)^2), \quad G(x, y, z, \epsilon, \mu) = \mathcal{O}(x, y, z, \epsilon),$$

and

$$H(x, y, z, \epsilon, \mu) = \mathcal{O}(xz, xy, z^2, \epsilon).$$

(In comparison with [34] we have zH instead of H . This plays little role, but the latter can be brought into the former by a transformation of x .) μ will be our bifurcation parameter.

The system is normalized in such a way that the layer problem has a critical manifold S of the form $x = m(y, z) := -z^2(1 + \mathcal{O}(y, z))$ with a fold along the line defined by $(0, y, 0)$. Locally, the manifold S is normally attracting along $z < 0$ and normally repelling along $z > 0$. Upon desingularization, the reduced problem takes the following form:

$$\begin{aligned} y' &= -z(1 + L(y, z, \mu))(\mu + 2G(m(y, z), y, z, 0, \mu)), \\ z' &= y - (\mu + 1)z + F(m(y, z), y, z, 0, \mu), \end{aligned} \tag{4}$$

with $x = m(y, z)$ and L smooth satisfying $L(0, 0, \mu) = 0$. Consequently, we have a folded singularity [39] at $(x, y, z) = (0, 0, 0)$. In fact, $(y, z) = (0, 0)$ is partially hyperbolic for (4) with $\mu = 0$ and a center manifold reduction shows that (4) undergoes a transcritical bifurcation for $\mu = 0$ if

$$\lambda := \partial_y G(\mathbf{0}) + \partial_z G(\mathbf{0}) \neq 0. \tag{5}$$

It is this bifurcation that is known as a folded saddle-node (of type II [34]) the slow-fast system (3). We illustrate the bifurcation in Fig. 1 in terms of the slow time; in comparison with (4) the directions on the repelling sheet are therefore reversed [39]. Here Fig. 1 (a) shows $\lambda < 0$ whereas Fig. 1 (b) shows $\lambda > 0$.

On the other hand, for each $\mu \sim 0$, there exists a strong stable manifold $\gamma_0(\mu)$ of $(y, z) = 0$ for (4), known as the strong singular canard in the (x, y, z) -space. It is well-known [39] that $\gamma_0(\mu)$ persists as a (maximal) canard $\gamma_\epsilon(\mu)$ connecting fixed copies of Fenichel slow manifolds $S_{a,\epsilon}$ and $S_{r,\epsilon}$ as perturbations of (appropriate) compact subsets $S_{a,0}$ and $S_{r,0}$ of $S_a := S \cap \{z < 0\}$ respectively $S_r := S \cap \{z > 0\}$ for all $0 < \epsilon \ll 1$.

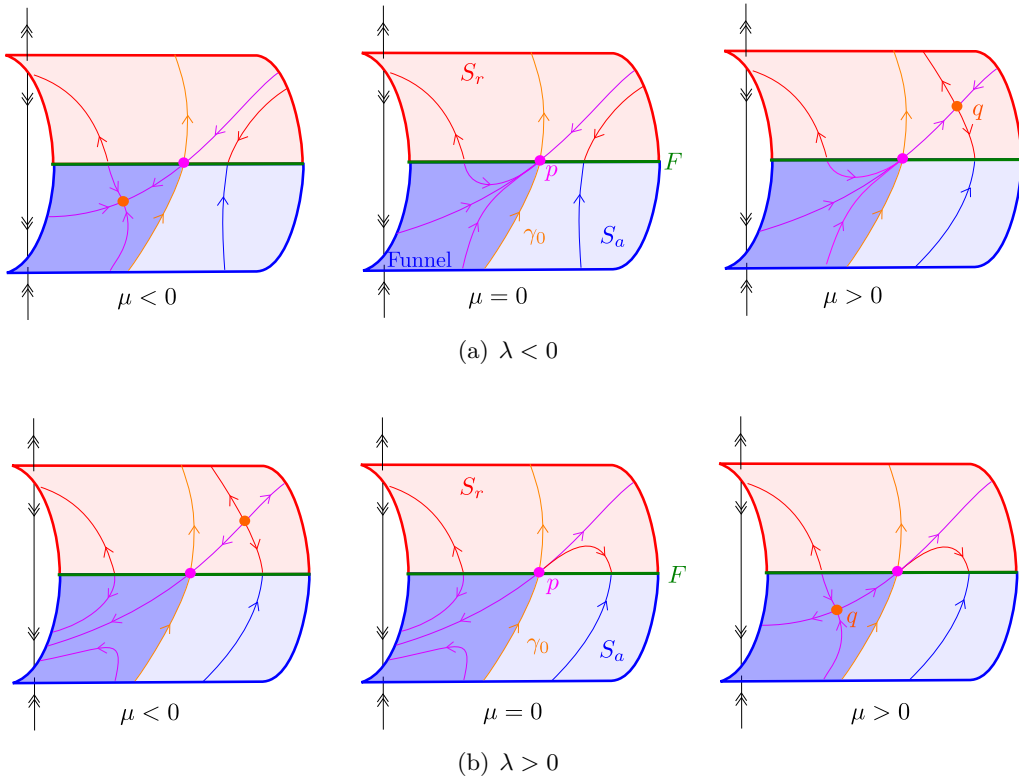


Figure 1: Illustration of the folded saddle-node of type II. It is a transcritical bifurcation of the desingularized reduced problem (4). The dynamics illustrated here is in terms of the slow time. Consequently, in comparison with (4), we have reversed the directions on the repelling sheet. The sign of λ (see (5)) determines on what side of the two sheets the saddle point q appears. For $\lambda < 0$, shown in (a), q lies on the repelling sheet C_r , appearing for $\mu \gtrsim 0$. For $\lambda > 0$, shown in (b), q lies on the attracting sheet C_a , appearing for $\mu \lesssim 0$. In both cases, the folded singularity p is a folded node on one side of μ and folded saddle on the other side. The strong singular canard $\gamma_0(\mu)$ divides C_a into separate sets. In particular, for $\mu \geq 0$ and $\lambda < 0$, the dark shaded region in (a) is a funnel region. Here all points pass through p upon following the reduced flow.

1.2 Main result

In this paper, we are interested in canard cycles, i.e. periodic orbits that follow $\gamma_0(\mu)$ on S . In particular, under the assumption (5) and analyticity of F , G and H , we prove the existence of a family of periodic orbits:

Theorem 1.1. *Suppose (5) and that F , G and H are analytic functions in the phase space variables x , y , z and smooth in ϵ and μ . Then there exists an $h_1 > 0$ such that for all $0 < \epsilon \ll 1$ the following holds: There is a Hopf bifurcation of (3) at $\mu = \mu_H(\sqrt{\epsilon})$, $\mu_H(0) = 0$, and a family of periodic orbits $\Gamma_{h,\epsilon}$, with $h \in (0, h_1]$ measuring the amplitude (to be defined later), along $\mu = \bar{\mu}(h, \epsilon)$, where $\bar{\mu}$ is continuous and satisfies $\bar{\mu}(0, \epsilon) = \mu_H(\sqrt{\epsilon})$. For each $h \in (0, h_1]$ fixed, $\Gamma_{h,\epsilon}$ converges as $\epsilon \rightarrow 0$ in Hausdorff distance to a singular canard cycle, consisting of a segment of $\gamma_0(\bar{\mu}(h, 0))$ across the fold and a fast jump. The limit is uniform on compact subsets of $(0, h_1]$.*

To prove Theorem 1.1, we follow [39], and apply the following blowup transformation to

the extended system $((3), \dot{\epsilon} = 0)$ of the folded singularity:

$$(r, (\bar{x}, \bar{y}, \bar{z}, \bar{\epsilon})) \mapsto \begin{cases} x &= r^2 \bar{x}, \\ y &= r \bar{y}, \\ z &= r \bar{z}, \\ \epsilon &= r^2 \bar{\epsilon}. \end{cases}$$

for $r \geq 0$, $(\bar{x}, \bar{y}, \bar{z}, \bar{\epsilon}) \in S^3$ and $\mu \sim 0$. In contrast to [34], we will not blowup $\mu = 0$ (at this stage, at least). We use two separate charts $\bar{x} = -1$ and $\bar{\epsilon} = 1$ with chart-specific coordinates $(\epsilon_1, r_1, y_1, z_1)$ and (r_2, x_2, y_2, z_2) defined by :

$$(\epsilon_1, r_1, y_1, z_1) \mapsto \begin{cases} x &= -r_1^2, \\ y &= r_1 y_1, \\ z &= r_1 z_1, \\ \epsilon &= r_1^2 \epsilon_1, \end{cases} \quad (6)$$

$$(r_2, x_2, y_2, z_2) \mapsto \begin{cases} x &= r_2^2 x_2, \\ y &= r_2 y_2, \\ z &= r_2 z_2, \\ \epsilon &= r_2^2, \end{cases} \quad (7)$$

respectively. The charts overlap on $\bar{x} < 0$ and here the change of coordinates are given by the expressions:

$$\begin{aligned} r_2 &= r_1 \sqrt{\epsilon_1}, \\ x_2 &= -\epsilon_1^{-1}, \\ y_2 &= y_1 / \sqrt{\epsilon_1}, \\ z_2 &= z_1 / \sqrt{\epsilon_1}, \end{aligned} \quad (8)$$

for $\epsilon_1 > 0$.

In [21, 34] the authors also describe the Hopf bifurcation in the $\bar{\epsilon} = 1$ -chart. The new contribution of Theorem 1.1 is that we describe the family of periodic orbits bifurcating from the Hopf in a full (i.e. ϵ -independent) neighborhood of the folded saddle-node for all $0 < \epsilon \ll 1$. This family includes periodic orbits with amplitude $h = \mathcal{O}(1)$ following the strong canard $\gamma_0(\mu)$ for $\mu \sim 0$ and all $0 < \epsilon \ll 1$.

Our approach is similar to the approach for the analysis of the canard explosion in the planar case, see [33]. The paper [33] also uses a Melnikov approach to extend the Hopf cycles in the associated scaling chart and then subsequently extend these to canard cycles by working in directional charts. The latter connection problem is already complicated in [33]. In the present paper, we feel that our proof in \mathbb{R}^3 is relatively simple. It basically extends the classical way of obtaining canard cycles in \mathbb{R}^2 , by flowing points forward and backward along the attracting and repelling sheets and then extending this close to the folded saddle-node through blowup (using the chart $\bar{x} = -1$). Shilnikov variables [12] and normal forms [22, 24] are used to study the necessary transition maps. This approach could also be used as an alternative to solving the connection problem in \mathbb{R}^2 , although we have not attempted to do so.

In contrast, the problem of connecting the Hopf cycles with the ones obtained by the Melnikov analysis is more complicated here in \mathbb{R}^3 than in the \mathbb{R}^2 -context of [33]. This is also related to our assumption on analyticity of F , G and H in Theorem 1.1, which may seem unusual for results in this direction. To explain the difficulty, we recall from [34] that

there is a critical manifold in the $\bar{\epsilon} = 1$ -chart for $\mu = r_2 = 0$ given by $x_2 = y_2^2, z_2 = y_2, y_2 \in \mathbb{R}$. The linearization has imaginary eigenvalues at $y_2 = 0$ and the reduced problem has a hyperbolic equilibrium precisely at this point; this is what produces the Hopf bifurcation for all $0 < r_2 \ll 1$. However, it is nontrivial to study the Hopf cycles in a fixed (small) neighborhood of the Hopf since the eigenvalues are of the form $\pm(1 + \mathcal{O}(r_2))i, r_2(\lambda + \mathcal{O}(r_2))$, i.e. a zero-Hopf bifurcation occurs at $\mu = r_2 = 0$. We find that there are two ways to perform the analysis of the Hopf cycles: (i) Perform a center manifold reduction and apply the Hopf bifurcation theorem there. Or: (ii) Straighten out the (strong) unstable/stable manifold ($\lambda \geq 0$, respectively), introduce polar coordinates in the transverse direction and apply Melnikov-like methods to construct the periodic orbits as fixed-points of a return map. However, both approaches are not uniform in $\epsilon \rightarrow 0$ in the smooth setting, due to the fact that the eigenvalue with the nonzero real part $\sim \epsilon\lambda$, providing the necessary hyperbolicity, goes to zero as $\epsilon \rightarrow 0$. Nevertheless, in the analytic case, we are able to extend the proof of the unstable/stable manifold to a fixed neighborhood (by following [11, Section 3]), and this allows us to apply approach (ii). In the author's opinion, there is no clear way to extend the proof of the unstable/stable in the smooth setting since this rests on the exponential estimates (that are nonuniform in the present context).

1.3 Overview

In the remainder of the paper, we work to prove Theorem 1.1. First in Section 2, we describe the small periodic orbits, extending all the way down to the Hopf bifurcation. Subsequently, in Section 3, we describe the ‘‘intermediate orbits’’ that connect small periodic orbits with the canard orbits. In Section 4, we complete the proof of the theorem. Finally, in Section 5 we conclude the paper through a discussion of the results and potential future work.

2 Existence of small periodic orbits

In the scaling chart $\bar{\epsilon} = 1$, applying (7) to $((3), \dot{\epsilon} = 0)$ gives

$$\begin{aligned}\dot{x}_2 &= y_2 - (\mu + 1)z_2 + r_2 F_2(x_2, y_2, z_2, r_2, \mu), \\ \dot{y}_2 &= \frac{1}{2}\mu + r_2 a_1 y_2 + r_2 a_2 z_2 + r_2^2 \bar{G}_2(x_2, y_2, z_2, r_2, \mu), \\ \dot{z}_2 &= x_2 + z_2^2 + r_2 z_2 H_2(x_2, y_2, z_2, r_2, \mu),\end{aligned}\tag{9}$$

and $\dot{r}_2 = 0$. Here the desingularization has been achieved by dividing the right hand side by r_2 . As in [34], we have put $a_1 = \partial_x G(\mathbf{0})$, $a_2 = \partial_z G(\mathbf{0})$. Recall then that

$$\lambda := a_1 + a_2 \neq 0,$$

by assumption (5). For $\mu \sim 0$, $r_2 \sim 0$ this system is slow-fast with x_2 and z_2 being fast and y_2 slow. In particular, $\mu = r_2 = 0$ gives an associated layer problem

$$\begin{aligned}\dot{x}_2 &= y_2 - z_2, \\ \dot{y}_2 &= 0, \\ \dot{z}_2 &= x_2 + z_2^2.\end{aligned}\tag{10}$$

Lemma 2.1. *The set C_2 defined by $x_2 = y_2^2, z_2 = y_2, y_2 \in \mathbb{R}$ is a critical manifold of (10). It is normally attracting for $y_2 < 0$ and repelling for $y_2 > 0$.*

On the other hand, $y_2 = 0$ is degenerate for C_2 with the linearization around $(0, 0, 0)$ having two imaginary eigenvalues $\pm i$. In particular, (10) is time-reversible within $y_2 = 0$ and the orbit

$$\gamma_{2,0}(0) : \begin{cases} x_2(t_2) &= -\frac{1}{4}t_2^2 + \frac{1}{2}, \\ z_2(t_2) &= \frac{1}{2}t_2, \end{cases} \quad (11)$$

is a separatrix in the (x_2, z_2) -plane separating closed periodic orbits $\phi_h(t) = (x_{2h}(t), z_{2h}(t))$, $x_{2h}(0) = -h, z_{2h}(0) = 0$ with period $T_0(h) > 0$ for any $h > 0$, from unbounded orbits.

Proof. The statement regarding the stability of C_2 follows from simple calculations. The analysis for $y_2 = 0$ is also straightforward, see [33]. \square

We illustrate the dynamics in the (x_2, z_2) -plane in Fig. 2.

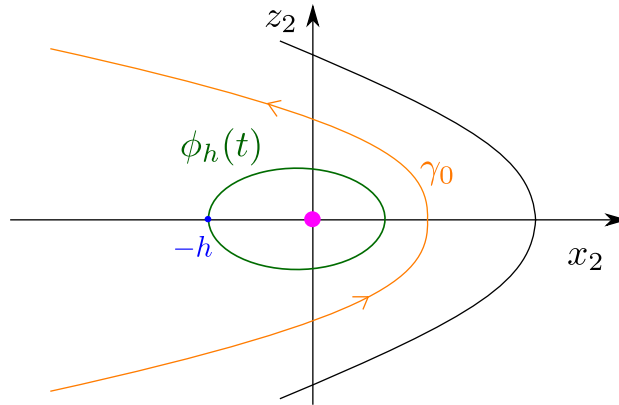


Figure 2: The layer problem (10) in the (x_2, z_2) -plane. The canard orbit γ_0 (orange) separates bounded periodic orbits ϕ_h (green) from unbounded orbits.

The solution (11) for $\mu = 0$ belongs to a μ -family of solutions

$$\gamma_{2,0}(\mu) : \begin{cases} x_2(t_2) &= -\frac{1}{4}t_2^2 + \frac{1}{2}, \\ y_2(t_2) &= \frac{\mu}{2}t_2, \\ z_2(t_2) &= \frac{1}{2}t_2, \end{cases} \quad (12)$$

of (9) for $\mu = r_2 = 0$. It corresponds to the blowup of the strong canard $\gamma_0(\mu)$, see [39].

To describe the reduced problem on C_2 , we consider the scaling

$$\mu = r_2 \mu_2. \quad (13)$$

Then with μ_2 fixed, $r_2 = 0$ implies $\mu = 0$. [34] also uses this scaling, but it is strictly speaking not necessary for the present analysis. In fact, it will be crucial to our approach not to scale μ for the description of the intermediate periodic orbits that we study later in the paper.

With (13), we obtain the following reduced problem on C_2 :

$$y_2' = \frac{1}{2}\mu_2 + \lambda y_2,$$

in terms of a slow time. For $\lambda \neq 0$, we have a hyperbolic equilibrium at

$$y_2 = -\frac{\mu_2}{2\lambda}. \quad (14)$$

Consequently, for $\mu_2 = 0$ this equilibrium lies at $y_2 = 0$, corresponding to the degenerate point of C_2 . This gives rise to the (singular) Hopf bifurcation [21].

As advertised in the introduction, we study the Hopf bifurcation and periodic orbits of (9) by first proving existence of a slow manifold Z_{2,r_2} (following [11, Section 3]), analytic in the space variables and smooth in ϵ and μ_2 , as a perturbation of C_2 in a fixed neighborhood of $y_2 = 0$. Then upon straightening out this one-dimensional manifold we ensure that polar coordinates in the normal directions are well-defined. This allows us to set up a return map, defined in a full neighborhood, which we describe using Melnikov theory.

2.1 Existence of an analytic slow manifold

It will be convenient to write $u := (x_2, z_2) \in \mathbb{R}^2$. Moreover, let $\Omega(\nu)$ for $\nu > 0$ denote the space of real-analytic functions $m : [-\nu, \nu] \rightarrow \mathbb{R}^2$. Then the following holds.

Proposition 2.2. *Fix $k \in \mathbb{N}$. Then there are constants $\delta > 0$ and $\nu > 0$, both sufficiently small, such that the following holds: There exists a locally invariant one-dimensional manifold Z_{2,r_2} of (9) of the graph form:*

$$u = m(y_2, r_2, \mu_2),$$

where $(r_2, \mu_2) \mapsto m(\cdot, r_2, \mu_2) \in \Omega(\nu)$ is C^k for $0 \leq r_2 \ll 1$, $\mu_2 \in [-\delta, \delta]$, satisfying $m(y_2, 0, \mu_2) = (y_2, y_2^2)$ such that $Z_{2,0}$ is a submanifold of C_2 .

Proof. It is elementary to transform the system into the following form:

$$\begin{aligned} \dot{\tilde{u}} &= A(v, \mu_2)\tilde{u} + r_2 R_2(\tilde{u}, v, r_2, \mu_2), \\ \dot{v} &= r_2 (v + r_2 P_2(\tilde{u}, v, r_2, \mu_2)), \end{aligned} \tag{15}$$

where $v = y_2 + \frac{1}{2\lambda}\mu_2$ and

$$A(v, \mu_2) = \lambda^{-1} \begin{pmatrix} 0 & -1 \\ 1 & 2v - \frac{1}{\lambda}\mu_2 \end{pmatrix}.$$

Henceforth we drop the tilde on u . The eigenvalues of $A(v, \mu_2)$ are $\pm\lambda^{-1}i + \mathcal{O}(v, \mu_2)$. Consequently, for all μ_2 sufficiently small, we have that

$$(qI - A(0, \mu_2))^{-1}$$

exists for all $q \in \mathbb{R}$.

Lemma 2.3. *Fix $\mu_2 \in [-\delta, \delta]$ with $\delta > 0$ sufficiently small. Then there exists a constant $C > 0$ such that*

$$\|(qI - A(0, \mu_2))^{-1}\| \leq \frac{C}{|q| + 1},$$

for all $q \in \mathbb{R}$ and all $\mu_2 \in [-\delta, \delta]$.

Proof. Clearly,

$$\|(qI - A(0, \mu_2))^{-1}\| \leq \tilde{C}|\chi(\mu_2) - q|^{-1},$$

where $\chi(\mu_2)$ and $\bar{\chi}(\mu_2)$ are the imaginary eigenvalues of $A(0, \mu_2)$. We then use that $\chi(\mu_2)$ is close to imaginary axes to obtain the result. \square

Henceforth we suppress the dependency of μ_2 . We then write the system as a first order system in the following form:

$$r_2 v \frac{du}{dv} - A(0)u = (A(v) - A(0))u + r_2 R_2(u, v, r_2) - r_2^2 P_2(u, v, r_2) \frac{du}{dv}. \quad (16)$$

We will solve this equation by using a fixed-point argument. For this purpose define the following Banach norm

$$\left\| \sum_{k=0}^{\infty} h_k v^k \right\| := \sum_{k=0}^{\infty} |h_k| \nu^k.$$

on the space $\Omega(\nu)$ of real analytic functions $h(v) = \sum_{k=0}^{\infty} h_k v^k \in \mathbb{R}^n$ with $\|h\| < \infty$ defined on $|v| \leq \nu$ with $\nu > 0$.

Now, consider first

$$r_2 v \frac{du}{dv} - A(0)u = F(v), \quad (17)$$

with $F := \sum_{k=0}^{\infty} F_k(\cdot)^k \in \Omega(\nu)$. Then we have the following:

Lemma 2.4. *Let $0 \leq r_2 \ll 1$ and define the linear operator $T_k : \mathbb{R}^2 \rightarrow \mathbb{R}^2$ by*

$$T_k(F_k) = (r_2 k - A(0))^{-1} F_k, \quad F_k \in \mathbb{R}^2.$$

Then

$$\|T_k\| \leq \frac{C}{r_2 k + 1}, \quad (18)$$

with $C > 0$ from Lemma 2.3 and

$$u(v) = T(F)(v) := \sum_{k=0}^{\infty} T_k(F_k) v^k, \quad (19)$$

is the unique real-analytic solution of (17) in $\Omega(\nu)$. The operator $T : \Omega(\nu) \rightarrow \Omega(\nu)$ defined by (19) is continuous:

$$\|T(F)\| \leq C \|F\|, \quad (20)$$

for all $F \in \Omega(\nu)$.

Proof. Straightforward. (18) follows from Lemma 2.3 which gives (20) upon using (19). \square

The following is also important.

Lemma 2.5. *Consider $F \in \Omega(\nu)$. Then*

$$\|T(r_2 F')\| \leq C \nu^{-1} \|F\|,$$

for all $0 < r_2 \ll 1$.

Proof. If $F(v) = \sum_{k=0}^{\infty} F_k v^k$ then $F'(v) = \sum_{k=0}^{\infty} (k+1)F_{k+1}v^k$. Consequently,

$$T(r_2 F')(v) = \sum_{k=0}^{\infty} T_k(r_2(k+1)F_{k+1})v^k,$$

and by Lemma 2.3:

$$\|T(r_2 F')\| \leq \sum_{k=0}^{\infty} \frac{Cr_2(k+1)}{r_2k+1} |F_{k+1}| \nu^k \leq C \sum_{k=0}^{\infty} |F_{k+1}| \nu^k \leq C\nu^{-1} \sum_{k=0}^{\infty} |F_k| \nu^k.$$

□

To solve (16), we therefore write it as a fixed-point equation:

$$u = \mathcal{L}(u),$$

where \mathcal{L} is the nonlinear operator defined by

$$\mathcal{L} : u \mapsto T \left((A(v) - A(0))u + r_2 R_2(u, v, r_2) - r_2^2 P_2(u, v, r_2) \frac{du}{dv} \right)$$

Consider the closed subset $\Omega_1(\nu, \sigma) \subset \Omega(\nu)$ defined by $\|m\| \leq \sigma$, $m \in \Omega(\nu)$.

Lemma 2.6. *There exist constants $\nu > 0$, $\sigma > 0$ and $r_{20} > 0$ such that \mathcal{L} is contraction on $\Omega_1(\nu, \sigma)$ for all $0 < r_2 \leq r_{20}$.*

Proof. The proof follows the proof of [11, Lemma 3.25], and we therefore leave out the full details. In fact, without the last term $r_2^2 P_2(u, v, r_2) \frac{du}{dv}$ the result is straightforward and obvious. We therefore only describe how to estimate the last term

$$T \left(r_2^2 P_2(u, v, r_2) \frac{du}{dv} \right),$$

cf. the linearity of T . For this we essentially follow the proof of Lemma 2.5: Write $P_2(u, v, r_2) = \sum_{n=0}^{\infty} P_{2,n}(r_2)v^n$ for $u = \sum_{k=0}^{\infty} h_k v^k$. Then

$$T \left(r_2^2 P_2 \frac{du}{dv} \right) = r_2^2 \sum_{k=0}^{\infty} T_k \left(\sum_{l=0}^{k+1} l h_l P_{2,k+1-l}(r_2) \right) v^k,$$

such that

$$\begin{aligned} \|T \left(r_2^2 P_2 \frac{du}{dv} \right)\| &\leq r_2 \sum_{k=0}^{\infty} \|T_k\| r_2(k+1) \sum_{l=0}^{k+1} |h_l| |P_{2,k+1-l}(r_2)| \nu^k \\ &\leq r_2 C \sum_{k=0}^{\infty} \sum_{l=0}^{k+1} |h_l| |P_{2,k+1-l}(r_2)| \nu^k \\ &\leq r_2 C \nu^{-1} \sum_{n=0}^{\infty} P_{2,n}(r_2) \nu^n \sum_{k=0}^{\infty} h_k \nu^k \\ &= r_2 C \nu^{-1} \|P_2\| \|u\|, \end{aligned}$$

which provides the essential estimate for showing that there are $\sigma > 0$ and $\nu > 0$ small enough, such that $\mathcal{L} : \Omega_1(\nu, \sigma) \rightarrow \Omega_1(\nu, \sigma)$ is well-defined for all $0 \leq r_2 \ll 1$. The Lipschitz constant of \mathcal{L} can be bounded from above by a constant $0 < c < 1$ in a similar way. □

By Banach's fixed point theorem, we obtain a unique fixed-point in $\Omega_1(\nu, \sigma)$. This fixed point $\tilde{u} = \tilde{m}(v, r_2, \mu_2)$ gives our desired locally invariant manifold of (15). Transforming the result back to the (x_2, y_2, z_2) -variables gives the desired result and completes the proof of Proposition 3.3. \square

The invariant manifold Z_{2,r_2} is a slow manifold extending uniformly with respect to r_2 across the degenerate set $y_2 = 0$, $\mu_2 = 0$. It is a subset of the stable (unstable) set of (14) for $\lambda < 0$ ($\lambda > 0$, respectively).

2.2 Melnikov theory

We now straighten out the slow manifold of Proposition 2.2 by writing:

$$\begin{pmatrix} x_2 \\ z_2 \end{pmatrix} = m(y_2, r_2, \mu_2) + \tilde{u}. \quad (21)$$

Then the invariant manifold corresponds to $\tilde{u} = 0$ and consequently:

$$\begin{aligned} \dot{\tilde{u}} &= B(\tilde{u}, y_2)\tilde{u} + r_2 R_2(\tilde{u}, y_2, r_2, \mu_2)\tilde{u}, \\ \dot{y}_2 &= r_2 \left(\frac{1}{2}\mu_2 + \lambda y_2 + P_2(\tilde{u}, y_2, r_2, \mu_2) \right), \end{aligned} \quad (22)$$

where $P_2(0, y_2, 0, \mu_2) = 0$ and

$$B(\tilde{u}, y_2) = \begin{pmatrix} 0 & -1 \\ 1 & 2y_2 + \tilde{u}_2 \end{pmatrix},$$

for $\tilde{u} = (\tilde{u}_1, \tilde{u}_2)$. For $r_2 = y_2 = 0$, we have $m(0, 0, \mu_2) = 0$ and hence \tilde{u} reduces to (x_2, z_2) in this case. We now again drop the tildes. The u -plane is therefore for $r_2 = 0$ also filled with the periodic orbits $\phi_h(t) = (x_{2h}(t), z_{2h}(t))$, intersecting the negative x_2 -axis in $(-h, 0)$ with $h > 0$. Moreover, due to the invariance of $u = 0$, the return map from $u_1 < 0, u_2 = 0$ to itself, mapping $(-h, 0, y_{20})$ to $(u_1(T), 0, y_2(T))$, with $T = T(h, y_2, r_2, \mu_2)$ being the transition time, is well-defined for all $h > 0$, $0 \leq r_2 \ll 1$, $\mu_2 \in [-\delta, \delta]$. In fact, polar coordinates in the u -plane is well-defined for all $y_2 \in [-\nu, \nu]$, $\mu_2 \in [-\delta, \delta]$, and as a result we obtain:

Lemma 2.7. *The return map has a smooth extension to $h = 0$ with $T(0, y_2, r_2, \mu_2) = 2\pi + \mathcal{O}(y_2, r_2)$.*

We now obtain fixed points of the return map using Melnikov theory to perturb away from the family of period orbits $u = \phi_h(t)$, $h > 0$, within $y_2 = 0$ for $\mu_2 = r_2 = 0$. For this purpose, let

$$A_h(t) := \begin{pmatrix} 0 & -1 \\ 1 & 2z_{2h}(t) \end{pmatrix},$$

denote the linearization around $u = \phi_h(t)$, $y_2 = r_2 = 0$. We then write

$$u = \phi_h(t) + \tilde{u}, \quad y_2 = \tilde{y}_2.$$

and let $\tilde{u}(t, h, y_2, r_2, \mu_2), \tilde{y}_2(t, h, y_2, r_2, \mu_2)$ denote the solutions of the resulting differential equations:

$$\begin{aligned} \dot{\tilde{u}} &= A_h(t)\tilde{u} + \left\{ B(\phi_h(t) + \tilde{u}, \tilde{y}_2)(\phi_h(t) + \tilde{u}) - A_h(t)\tilde{\phi}_h(t) - A_h(t)\tilde{u} \right. \\ &\quad \left. + r_2 R_2(\phi_h(t) + \tilde{u}, \tilde{y}_2, r_2, \mu_2)(\phi_h(t) + \tilde{u}) \right\}, \\ \dot{\tilde{y}}_2 &= r_2 \left(\frac{1}{2}\mu_2 + \lambda\tilde{y}_2 + P_2(\phi_h(t) + \tilde{u}, \tilde{y}_2, r_2, \mu_2) \right), \end{aligned}$$

with initial conditions $\tilde{u}(0) = 0, \tilde{y}_2(0) = y_2$. We have

$$\tilde{u}(t, 0, y_2, r_2, \mu_2) \equiv 0,$$

due to $\phi_0(t) \equiv 0$ and the invariance of $u = 0$ for (22). Let $\Phi_h(t, s)$ denote the state-transition matrix associated with $A_h(t)$. Then by variation of constants we have that

$$\begin{aligned}\tilde{u}(T, h, y_2, r_2, \mu_2) &= \int_0^T \Phi_h(T, t) \{\cdots\} dt, \\ \tilde{y}_2(T, h, y_2, r_2, \mu_2) &= y_2 + \int_0^T r_2(\cdots) dt,\end{aligned}$$

where

$$\begin{aligned}\{\cdots\} &= B(\phi_h(t) + \tilde{u}(T, h, y_2, r_2, \mu_2), \tilde{y}_2)(\phi_h + \tilde{u}(t, h, y_2, r_2, \mu_2)) - A_h(t)\tilde{\phi}_h(t) \\ &\quad - A_h(t)\tilde{u}(t, h, y_2, r_2, \mu_2) + r_2 R_2(\phi_h(t) + \tilde{u}(t, h, y_2, r_2, \mu_2), \tilde{y}_2(t, h, y_2, r_2, \mu_2), r_2, \mu_2) \\ &\quad \times (\phi_h(t) + \tilde{u}(t, h, y_2, r_2, \mu_2)), \\ (\cdots) &= \frac{1}{2}\mu_2 + \lambda\tilde{y}_2(t, h, y_2, r_2, \mu_2) + P_2(\phi_h(t) + \tilde{u}(t, h, y_2, r_2, \mu_2), \tilde{y}_2(t, h, y_2, r_2, \mu_2), r_2, \mu_2).\end{aligned}$$

Recall that $T(h, y_2, r_2, \mu_2)$ denotes the transition time, with $T_0(h) := T(h, 0, 0, 0)$ being the period of the periodic orbits $\phi_h(t) = (x_{2h}(t), z_{2h}(t))$. Since the eigenvalues of $B(0, 0)$ are $\pm i$, we have

$$\phi_h(t) = -h \begin{pmatrix} \cos t + \mathcal{O}(h) \\ \sin t + \mathcal{O}(h) \end{pmatrix}, \quad (23)$$

for $h \rightarrow 0^+$. Moreover:

$$T_0(0) := \lim_{h \rightarrow 0^+} T_0(h) = 2\pi, \quad (24)$$

see also Lemma 2.7. We then consider the adjoint system:

$$\dot{\psi} = -A_h(t)^T \psi,$$

and let $\psi_h(t)$ denote the solution with $\psi_h(T) = (1, 0)$. Then a simple calculation shows the following:

Lemma 2.8.

$$\psi_h(t) = -h^{-1} e^{\int_t^T 2z_{2h}(s) ds} \begin{pmatrix} z'_{2h}(t) \\ -x'_{2h}(t) \end{pmatrix}.$$

Moreover,

$$\psi_h(T) \cdot \tilde{u}(T, h, y_2, r_2, \mu_2) = \int_0^T \psi_h(t) \cdot \{\cdots\} dt. \quad (25)$$

Proof. This is standard and follows from the theory of adjoint equations, see [36]. In particular, for (25) we use $\psi_h(T)^T \Phi_h(T, s) = \psi_h(s)^T$. \square

We therefore define the Melnikov functions

$$\begin{aligned}\Delta_1(h, y_2, r_2, \mu_2) &= [x_{2h}(T) - h] + \int_0^T \psi_h(t) \cdot \{\dots\} dt, \\ \Delta_2(h, y_2, r_2, \mu_2) &= \int_0^T (\dots) dt.\end{aligned}$$

so that roots of $\Delta := (\Delta_1, \Delta_2)$ for $h > 0$ correspond to fixed points of the return map and periodic orbits. We have:

Lemma 2.9. Δ also extends smoothly to $h = 0$, with $\Delta_1(0, y_2, r_2, \mu_2) \equiv 0$ and $\Delta(h, 0, 0, 0) \equiv 0$ for all $h \geq 0$.

Proof. The extension of Δ follows from the invariance of $u = 0$ of (22) and the fact that T extends smoothly to $h = 0$, recall Lemma 2.7. The invariance of $u = 0$ and the fact that $\phi_0(t) \equiv 0$ also gives $\{\dots\} = 0$ for $h = 0$ and therefore $\Delta_1(0, y_2, r_2, \mu_2) \equiv 0$. Finally, $\Delta(h, 0, 0, 0) = 0$ since $u = (x_2, z_2) = \phi_h(t)$ is a solution of (10) within $y_2 = 0$ and $r_2 = 0$. \square

Following this lemma, the function

$$\widehat{\Delta} := (h^{-1}\Delta_1, \Delta_2),$$

is well-defined and smooth on $h \geq 0$. Moreover:

Lemma 2.10. $\widehat{\Delta}(h, 0, 0, 0) \equiv 0$ and

$$\widehat{\Delta}'_{y_2}(h, 0, 0, 0) = \begin{pmatrix} -2 \int_0^{T_0(h)} e^{\int_t^T 2z_{2h}(s)ds} (h^{-1}z_{2h})(t)^2 dt \\ * \end{pmatrix}, \quad (26)$$

$$\widehat{\Delta}'_{\mu_2}(h, 0, 0, 0) = \begin{pmatrix} 0 \\ \frac{1}{2}T_0(h) \end{pmatrix}, \quad (27)$$

for all $h \geq 0$, with $*$ denoting a quantity that is not important.

Proof. $\widehat{\Delta}(h, 0, 0, 0) \equiv 0$ follows from Lemma 2.9 and (27) is obvious. To show (26), we compute for $h > 0$:

$$\begin{aligned}\frac{\partial \Delta_1}{\partial y_2}(h, 0, 0, 0) &= \int_0^{T_0} \psi_h(t) \cdot \begin{pmatrix} 0 & 0 \\ 0 & 2 \end{pmatrix} \phi_h(t) dt \\ &= 2h^{-1} \int_0^T e^{\int_t^T 2z_{2h}(s)ds} x'_{2h}(t) z_{2h}(t) dt \\ &= -2h^{-1} \int_0^T e^{\int_t^T 2z_{2h}(s)ds} z_{2h}(t)^2 dt.\end{aligned}$$

$h^{-1}z_{2h}$ extends to all $h \geq 0$ by (23), which then completes the proof. \square

The Jacobian matrix

$$\widehat{\Delta}'_{(y_2, \mu_2)}(h, 0, 0, 0) := \begin{pmatrix} \widehat{\Delta}'_{y_2}(h, 0, 0, 0) & \widehat{\Delta}'_{\mu_2}(h, 0, 0, 0) \end{pmatrix},$$

is therefore regular for all $h > 0$, regardless of what $*$ is, also for $h = 0$ due to (23) and (24):

$$\widehat{\Delta}'_{y_2}(\mathbf{0}) = \begin{pmatrix} -2\pi \\ * \end{pmatrix}, \quad \widehat{\Delta}'_{\mu_2}(\mathbf{0}) = \begin{pmatrix} 0 \\ \pi \end{pmatrix}.$$

Proposition 2.11. Fix any $h_1 > 0$. Then there exist smooth functions $\bar{y}_2(h, r_2), \bar{\mu}_2(h, r_2)$ with $\bar{y}_2(h, 0) = 0, \bar{\mu}_2(h, 0) = 0$ such that $\widehat{\Delta}(h, \bar{y}_2(h, r_2), r_2, \bar{\mu}_2(h, r_2)) = 0$ for all $h \in [0, h_1]$ and all $0 \leq r_2 \ll 1$.

Proof. Follows from the implicit function theorem. \square

Corollary 2.12. Let $\mu_H(r_2) := r_2 \bar{\mu}_2(0, r_2)$. Then (9) undergoes a Hopf bifurcation at $\mu = \mu_H(r_2)$ for $0 < r_2 \ll 1$.

Proof. The statement follows directly from Proposition 2.11. \square

Remark 2.13. We do not aim to describe the stability of the cycles. This is more difficult. However, sufficiently close to the Hopf bifurcation, one can describe stability in terms of the signs of λ and $\frac{\partial^2 \bar{\mu}_2}{\partial h^2}(0, r_2)$; here the latter quantity relates directly to the first Lyapunov coefficient of the Hopf (within a center manifold). In particular, if $\lambda > 0$ then $\mu_2 \geq \mu_H(r_2)$ means that the equilibrium is on the attracting/repelling side of Z_{2, r_2} , respectively. Therefore sufficiently close to the equilibrium, the limit (Hopf) cycles are unstable/stable if $\frac{\partial^2 \bar{\mu}_2}{\partial h^2}(0, r_2) \geq 0$ for $\lambda > 0$. If $\lambda < 0$, then the inequalities for μ_2 regarding the “normal stability” of (14) become $\mu_2 \leq \mu_H(r_2)$ and the Hopf cycles are unstable/stable if $\frac{\partial^2 \bar{\mu}_2}{\partial h^2}(0, r_2) \leq 0$ in this case.

It is possible to compute a leading order expression for $\frac{\partial^2 \bar{\mu}_2}{\partial h^2}(0, r_2)$ but we chose not to include the complicated expression in the present paper.

Obviously, one could just compute the Lyapunov coefficient by applying the center manifold reduction, see [21]. But – due the zero-Hopf bifurcation for $r_2 = 0$ – this approach does not guarantee that this quantity describe the stability of limit cycles in a uniform neighborhood. Our Melnikov approach using Proposition 3.3 in the analytic setting does imply such uniformity.

The family of periodic orbits of (9) are small periodic orbits (with amplitude of order $o(1)$) of (3) upon *blowing down* using (7). By working in the chart $\bar{x} = -1$ in the following section, we are able to extend these cycles to “intermediate” cycles that include $\mathcal{O}(1)$ canards.

3 Existence of intermediate periodic orbits

Our strategy for extending the small periodic orbits to intermediate ones, that connect to cycles of size $\mathcal{O}(1)$, follows the approach for proving canard cycles in \mathbb{R}^2 : Working in the entry chart $\bar{x} = -1$, we fix a section along $z_1 = 0$, in a neighborhood of $(r_1, y_1, \epsilon_1) = 0$ with $\mu \sim 0$, and flow the points forward and backward and then measure their separation on a section $\{z_2 = 0\}$ in the scaling chart $\bar{\epsilon} = 1$ transverse to $\gamma_{2,0}(0)$, recall (11). Based upon expansions from the solution of a Shilnikov problem [12], we define appropriate scalings that allow us to solve for roots of the separation function by applying the implicit function theorem.

3.1 Analysis in the $\bar{x} = -1$ -chart

We first consider the $\bar{x} = -1$ -chart. Inserting (6) into ((3), $\dot{c} = 0$) gives

$$\begin{aligned}\dot{\epsilon}_1 &= \epsilon_1^2 [y_1 - (\mu + 1)z_1 + r_1 F_1(\epsilon_1, r_1, y_1, z_1, \mu)], \\ \dot{r}_1 &= -\frac{1}{2}r_1\epsilon_1 [y_1 - (\mu + 1)z_1 + r_1 F_1(\epsilon_1, r_1, y_1, z_1, \mu)], \\ \dot{y}_1 &= \epsilon_1 \left(\frac{1}{2}\mu + r_1 G_1(\epsilon_1, r_1, y_1, z_1, \mu) \right) + \frac{1}{2}\epsilon_1 y_1 [y_1 - (\mu + 1)z_1 + r_1 F_1(\epsilon_1, r_1, y_1, z_1, \mu)], \\ \dot{z}_1 &= -1 + z_1^2 + r_1 z_1 H_1(\epsilon_1, r_1, y_1, z_1, \mu) + \frac{1}{2}\epsilon_1 z_1 [y_1 - (\mu + 1)z_1 + r_1 F_1(\epsilon_1, r_1, y_1, z_1, \mu)],\end{aligned}\tag{28}$$

where $F_1 = r_1^{-2}F$, $G_1 = r_1^{-2}G$, and $H_1 = r_1^{-2}H$, each being smooth, also upon extending to $r_1 = 0$. The points $(0, 0, y_1, -1)$ are partially attracting, whereas $(0, 0, y_1, 1)$ are partially repelling. In particular, in each case the linearization has a single nonzero eigenvalue (positive/negative, respectively). Consequently, by center manifold theory we have the following.

Lemma 3.1. *There exists a constant $\sigma > 0$ sufficiently small such that the following holds: There exist two three-dimensional center manifolds $M_{1,a}$ and $M_{1,r}$ of the sets $(0, 0, y_1, -1)$ and $(0, 0, y_1, 1)$, $y_1 \in [-\sigma, \sigma]$, having the following graph representations:*

$$\begin{aligned}M_{1,a} : \quad z_1 &= m_{1,a}(\epsilon_1, r_1, y_1, \mu), \\ M_{1,r} : \quad z_1 &= m_{1,r}(\epsilon_1, r_1, y_1, \mu),\end{aligned}$$

for $0 \leq r_1, \epsilon_1, |y_1|, |\mu| \leq \sigma$. The functions $m_{1,a}$ and $m_{1,r}$ are smooth functions on the specified domain and satisfy $m_{1,a}(0, 0, y_1, \mu) \equiv -1$, $m_{1,r}(0, 0, y_1, \mu) \equiv 1$ for all $y_1, \mu \in [-\sigma, \sigma]$ as well as

$$m_{1,a}(\epsilon_1, 0, \pm\mu, \mu) \equiv -1, m_{1,r}(\epsilon_1, 0, \pm\mu, \mu) \equiv 1.\tag{29}$$

The properties in (29) are consequences of the invariant sets $\gamma_{2,0}(\mu)$ in the $\bar{e} = 1$ -chart, recall (12), which in the present chart become $r_1 = 0, y_1 = \mp\mu, z_1 = \mp 1$ and $\epsilon_1 \geq 0$; we denote these sets by $\gamma_{1,0,a}(\mu)$ and $\gamma_{1,0,r}(\mu)$, respectively. We illustrate the dynamics in the $\bar{x} = -1$ -chart in Fig. 3.

As is standard, the center manifolds $M_{1,a}, M_{1,r}$ provide extensions of the family of Fenichel slow manifolds $\{(S_{a,\epsilon}, \epsilon) : \epsilon \in [0, \epsilon_0]\}$ as ((3), $\dot{c} = 0$) as foliations (through $r_1^2 \epsilon_1 = \epsilon = \text{const.}$) of the center manifolds [15].

On $M_{1,a}$ and $M_{1,r}$ we have the following desingularized reduced problems

$$\begin{aligned}\epsilon_1' &= \epsilon_1, \\ r_1' &= -\frac{1}{2}r_1, \\ y_1' &= \frac{\frac{1}{2}\mu + \mathcal{O}(r_1)}{y_1 + (\mu + 1) + \mathcal{O}(\epsilon_1, r_1)} + \frac{1}{2}y_1,\end{aligned}\tag{30}$$

and

$$\begin{aligned}\epsilon_1' &= -\epsilon_1, \\ r_1' &= \frac{1}{2}r_1, \\ y_1' &= \frac{\frac{1}{2}\mu + \mathcal{O}(r_1)}{-y_1 + (\mu + 1) + \mathcal{O}(\epsilon_1, r_1)} - \frac{1}{2}y_1,\end{aligned}\tag{31}$$

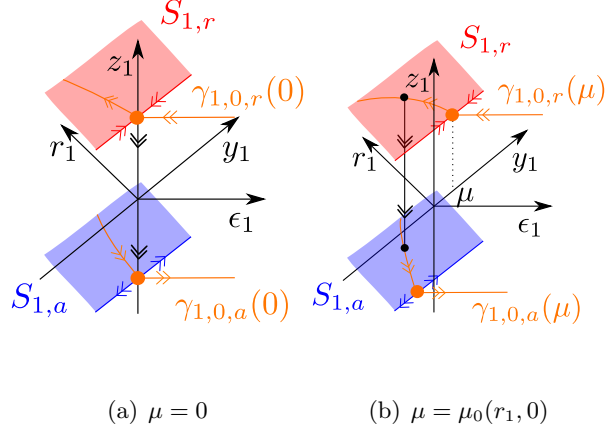


Figure 3: Dynamics in the entry chart $\bar{x} = -1$. In (a): for $\mu = 0$. In (b): for $\mu = \mu_0(r_1, 0)$. μ_0 is defined later, but essentially $\mu_0(\tilde{r}_1, 0)$ with $\tilde{r}_1 > 0$ is so that for $r_1 = \tilde{r}_1$, $\mu = \mu(\tilde{r}_1, 0)$ there is fast jump connecting γ_0 to itself.

obtained by dividing the right hand sides by $\pm\epsilon_1 [y_1 - (\mu + 1)z_1 + r_1 F_1(\epsilon_1, r_1, y_1, z_1, \mu)]$ and then substituting $z_1 = m_{1,a}(\dots)$ and $z_1 = m_{1,r}(\dots)$, respectively. Notice that the square brackets $\pm [y_1 - (\mu + 1)z_1 + r_1 F_1(\epsilon_1, r_1, y_1, z_1, \mu)]$ are positive near $M_{1,a}$ and $M_{1,r}$, respectively, and for $\epsilon_1 > 0$ the divisions therefore correspond to time transformations.

The system (30) has a hyperbolic equilibrium at $(0, 0, -\mu)$ with eigenvalues $-1/2, 1, \lambda(\mu)$ where

$$\lambda(\mu) = \frac{1}{2}(1 - \mu). \quad (32)$$

Similarly, (31) has a hyperbolic equilibrium at $(0, 0, \mu)$ with eigenvalues $\frac{1}{2}, -1, -\lambda(\mu)$. There are therefore strong resonances of both systems when $\mu = 0$.

In the following, we now describe two transition mappings $P_{1,a}$ and $P_{1,r}$ from $\{z_1 = 0\}$ to $\{\epsilon_1 = \epsilon_{11}\}$ obtained by applying the forward and backward flow, respectively. See illustration in Fig. 3. We will describe each mapping in appropriate “normal form coordinates”. Since the two mappings are similar, we focus on $P_{1,a}$.

Lemma 3.2. *Consider (28) near $M_{1,a}$. Then for $\sigma > 0$ small enough, there exists a regular transformation of time and a smooth diffeomorphism $(y_1, z_1) \mapsto (y_{1,a}, z_{1,a})$, $y_1, z_1 + 1 \in [-\sigma, \sigma]$, depending smoothly on (ϵ_1, r_1, μ) for $0 \leq r_1, \epsilon_1, |\mu| \leq \sigma$, such that*

$$\begin{aligned} y_{1,a} &= h_{1,a}^0(\epsilon_1, r_1, y_1, \mu) + \epsilon_1 h_{1,a}^1(\epsilon_1, r_1, y_1, z_1, \mu), \\ z_{1,a} &= z_1 - m_{1,a}(\epsilon_1, r_1, y_1, \mu), \end{aligned} \quad (33)$$

where

$$h_{1,a}^0(\epsilon_1, 0, -\mu, \mu) \equiv 0, \quad \frac{\partial h_{1,a}^0}{\partial y_1}(\mathbf{0}) = 1, \quad \frac{\partial h_{1,a}^0}{\partial \mu}(\mathbf{0}) = 1, \quad (34)$$

and (28) becomes

$$\begin{aligned} \dot{\epsilon}_1 &= \epsilon_1^2, \\ \dot{r}_1 &= -\frac{1}{2}r_1\epsilon_1, \\ \dot{y}_{1,a} &= ((\lambda(\mu) + r_1 L_0(r_1, y_{1,a}, \mu))y_{1,a} + r_1\epsilon_1 L_1(\epsilon_1, r_1, y_{1,a}, \mu))\epsilon_1, \\ \dot{z}_{1,a} &= (-2 + L_2(r_1, y_{1,a}, z_{1,a}, \epsilon_1, \mu))z_{1,a}, \end{aligned} \quad (35)$$

with L_0, L_1, L_2 each smooth and $L_2(\mathbf{0}) = 0$.

Proof. We first divide the right hand side by

$$y_1 - (\mu + 1)z_1 + r_1 F_1(\epsilon_1, r_1, y_1, z_1, \mu),$$

which is positive near $M_{1,a}$. This defines our regular transformation of time. Consequently,

$$\begin{aligned}\dot{\epsilon}_1 &= \epsilon_1^2, \\ \dot{r}_1 &= -\frac{1}{2}r_1\epsilon_1, \\ \dot{y}_1 &= \frac{\epsilon_1 \left(\frac{1}{2}\mu + r_1 G_1(\epsilon_1, r_1, y_1, z_1, \mu) \right)}{y_1 - (\mu + 1)z_1 + r_1 F_1(\epsilon_1, r_1, y_1, z_1, \mu)} + \frac{1}{2}\epsilon_1 y_1, \\ \dot{z}_1 &= -1 + z_1^2 + r_1 z_1 H_1(\epsilon_1, r_1, y_1, z_1, \mu) + \frac{1}{2}\epsilon_1 z_1,\end{aligned}$$

We then rectify $M_{1,a}$ to $z_{1,a} = 0$ by $z_1 = m_{1,a}(\epsilon_1, r_1, y_1, \mu) + z_{1,a}$ and subsequently straighten out the associated stable fibers of $M_{1,a}$ by a near-identity transformation $(\epsilon_1, r_1, y_1, z_{1,a}, \mu) \mapsto \tilde{y}_1$ such that $(\epsilon_1, r_1, \tilde{y}_1)'$ becomes independent on $z_{1,a}$ [27, 26]. Then

$$\begin{aligned}\dot{\epsilon}_1 &= \epsilon_1^2, \\ \dot{r}_1 &= -\frac{1}{2}r_1\epsilon_1, \\ \dot{\tilde{y}}_1 &= \epsilon_1 \left(\frac{\frac{1}{2}\mu + \mathcal{O}(r_1)}{\tilde{y}_1 + (\mu + 1) + \mathcal{O}(\epsilon_1, r_1)} + \frac{1}{2}\tilde{y}_1 \right), \\ \dot{z}_{1,a} &= (-2 + \mathcal{O}(\epsilon_1, r_1, \tilde{y}_1, z_{1,a}, \mu))z_{1,a}.\end{aligned}$$

By construction $r_1, \epsilon_1, \tilde{y}_1$ decouples. For $\epsilon_1 = 0$ it easy to see that $\tilde{y}_1 = y_1$. This shows the form of (33) with the z_1 -dependency of $y_{1,a}$ only entering the $\mathcal{O}(\epsilon_1)$ -term. Indeed, in the remainder of the proof we only transform \tilde{y}_1 in order to normalize the reduced problem on $z_{1,a} = 0$:

$$\begin{aligned}\epsilon_1' &= \epsilon_1, \\ r_1' &= -\frac{1}{2}r_1, \\ y_1' &= \frac{\frac{1}{2}\mu + \mathcal{O}(r_1)}{y_1 + (\mu + 1) + \mathcal{O}(\epsilon_1, r_1)} + \frac{1}{2}y_1,\end{aligned}\tag{36}$$

after dividing the right hand side by ϵ_1 . We have here dropped the tilde on y_1 and the system then coincides (by construction) with (30).

Put $y_1 = -\mu + \tilde{y}_1$. Then

$$\begin{aligned}\epsilon_1' &= \epsilon_1, \\ r_1' &= -\frac{1}{2}r_1, \\ y_1' &= \lambda(\mu)y_1 + L_1(\epsilon_1, r_1, y_1, \mu),\end{aligned}$$

after dropping the tildes, with $L_1(\cdot, \mu)$ being of second order. First consider the $r_1 = 0$ sub-system. This system can be smoothly linearized by a transformation of the form $(\epsilon_1, y_1, \mu) \mapsto \tilde{y}_1 = h_{1,a}(\epsilon_1, y_1, \mu)$ with $h_{1,a}(0, 0, \mu) = 0$, $\frac{\partial h_{1,a}}{\partial y_1}(0, 0, \mu) = 1$, see [14, 24]. Applying this transformation to the full system, we may take L_1 to be of the form $L_1 = r_1 \tilde{L}_1$. Then within

$\epsilon_1 = 0$, we have a saddle for $\mu \sim 0$ and we can straighten out the unstable manifold by an r_1 -dependent transformation of y_1 : $(r_1, y_1) \mapsto y_{1,a}$. This gives $\tilde{L} = y_{1,a}\tilde{L}_0 + \epsilon_1\tilde{L}_1$:

$$\begin{aligned} \epsilon'_1 &= \epsilon_1, \\ r'_1 &= -\frac{1}{2}r_1, \\ y'_{1,a} &= (\lambda(\mu) + r_1L_0(r_1, y_{1,a}, \mu))y_{1,a} + r_1\epsilon_1L_1(\epsilon_1, r_1, y_{1,a}, \mu), \end{aligned} \tag{37}$$

upon dropping the tildes. This completes the proof. \square

Since the flow is regular on sets that are uniformly bounded away from $M_{1,a}$ and $M_{1,r}$, we can actually extend the transformation leading to (35) to $z_1 \in [-1 - \sigma, 0]$, say, by the flow-box theorem. We therefore describe $P_{1,a}$ using the coordinates of (35) from $\{z_{1,a} = -\tilde{m}_{1,a}(\epsilon_1, r_1, y_{1,a}, \mu)\}$ to $\{\epsilon_1 = \epsilon_{11}\}$. Here $\tilde{m}_{1,a}(\epsilon_1, r_1, y_{1,a}, \mu) := m_{1,a}(r_1, y_1(\epsilon_1, r_1, y_{1,a}, \mu), \epsilon_1, \mu)$ with the smooth function $y_1(\epsilon_1, r_1, y_{1,a}, \mu)$ being obtained (by the implicit function theorem) from (33) with $z_1 = 0$:

$$y_{1,a} = h_{1,a}^0(\epsilon_1, r_1, y_1, \mu) + \epsilon_1 h_{1,a}^1(\epsilon_1, r_1, y_1, 0, \mu).$$

For simplicity, we denote the transformed mapping

$$P_{1,a}(\epsilon_1, r_1, y_{1,a}, \mu) = \begin{pmatrix} \epsilon_{11} \\ \sqrt{\epsilon_1 \epsilon_{11}^{-1} r_1} \\ * \\ * \end{pmatrix},$$

by the same symbol. Notice that the r_1 - and ϵ_1 -components of the mapping are just consequences of the conservation of $\epsilon = r_1^2 \epsilon_1$.

We describe $P_{1,a}$ in Proposition 3.4, but in preparation we first state a result on the *Shilnikov problem* associated with the $(\epsilon_1, r_1, y_{1,a})$ -subsystem, written in the desingularized form (37). For this, it will be convenient to work with functions $(u, v) \in U \times V \mapsto f(u, v) \in \mathbb{R}^l$, $U \subset \mathbb{R}^n, V \subset \mathbb{R}^m, l, n, m \in \mathbb{N}$, that are C^k -smooth, $k \in \mathbb{N}$, with respect to the $v \in V$, depending continuously on $u \in U$. We write the function space of such functions by $C(u^0 v^k)$ and let

$$\|f\|_{u^0 v^k} := \sup_{(u,v) \in U \times V, 0 \leq |i| \leq k} |D^i f(u, v)|,$$

with D^i being the partial derivative with respect to v of order $i = (i_1, \dots, i_m) \in \mathbb{N}_0^m$, denote the associated Banach norm. Notice that by $C(u^0 v^k)$ and $\|\cdot\|_{u^0 v^k}$ we suppress l, n, m, U and V ; it should be clear from the context what these are. On the other hand, we use $\|f\|_{C^k} := \sup_{u \in U, 0 \leq |i| \leq k} |D^i f(u)|$ to denote the usual C^k -norm of a C^k -smooth function $f : U \rightarrow \mathbb{R}^l$.

Proposition 3.3. *Fix $k \in \mathbb{N}$ and consider (37). Then there exist constants $\tau_0 > 0, K > 0$ and $C > 0$ such that the following holds for all $\delta > 0$ small enough: There exists a C^k -smooth function $\underline{y}_{1,a}(t, \tau, \epsilon_{11}, r_{10}, y_{11}, \mu)$, defined on the set given by: $(t, \tau) : 0 \leq t \leq \tau, \tau > \tau_0$ and $0 \leq \epsilon_{11}, r_{10}, |y_{11}|, |\mu| \leq K\delta$, such that $y_{1,a}(t) = \underline{y}_{1,a}(t, \tau, \epsilon_{11}, r_{10}, y_{11}, \mu)$ solves the Shilnikov problem defined by*

$$\epsilon_1(\tau) = \epsilon_{11}, \quad r_1(0) = r_{10}, \quad y_{1,a}(\tau) = y_{11}.$$

Moreover, $\underline{y}_{1,a}$ has the following expansion:

$$\underline{y}_{1,a}(t, \tau, \epsilon_{11}, r_{10}, y_{11}, \mu) = e^{\lambda(\mu)(t-\tau)}(y_{11} + \phi(t, \tau, \epsilon_{11}, r_{10}, y_{11}, \mu)),$$

where $\|\phi\|_{C^k} \leq C$; specifically

$$\|\phi\|_{(t,\tau,\epsilon_{11},r_{10})^0(y_{11},\mu)^k} \leq \delta, \quad \phi(t, \tau, \epsilon_{11}, 0, 0, \mu) \equiv 0. \quad (38)$$

Proof. The proof follows [12] and we therefore delay the details to Appendix A. \square

Proposition 3.4. Fix $k \in \mathbb{N}$ and any $\delta > 0$. Then there exist constants $c > 0$, $\chi > 0$ and $0 < \epsilon_{10} \ll \epsilon_{11}$, $r_{10} > 0$ such that the following holds: The transition map $P_{1,a}(\cdot, \mu)$ of (35) is well-defined on a region $V_{1,a}(\chi)$ defined by

$$|y_{1,a}| \leq \chi(\epsilon_1 \epsilon_{11}^{-1})^{\lambda(\mu)}, \epsilon_1 \in [0, \epsilon_{10}], r_1 \in [0, r_{10}], \quad (39)$$

and on this region, the mapping takes the following form

$$P_{1,a}(\epsilon_1, r_1, y_{1,a}, \mu) = \begin{pmatrix} \frac{\epsilon_{11}}{\sqrt{\epsilon_1 \epsilon_{11}^{-1} r_1}} \\ (\epsilon_1^{-1} \epsilon_{11})^{\lambda(\mu)} y_{1,a} + \psi_{1,a}(\epsilon_1, r_1, (\epsilon_1^{-1} \epsilon_{11})^{\lambda(\mu)} y_{1,a}, \mu) \\ \mathcal{O}(e^{-c/\epsilon_1}) \end{pmatrix}.$$

Here $\psi_{1,a}$ is a $C(\epsilon_1^0(r_1, u, \mu)^k)$ -function on the set $r_1 \in [0, r_{10}], \epsilon_1 \in [0, \epsilon_{10}], 0 \leq |u|, |\mu| \leq \chi$ with

$$\|\psi_{1,a}\|_{(\epsilon_1, r_1)^0(u, \mu)^k} \leq \delta, \quad \psi_{1,a}(\epsilon_1, 0, 0, \mu) \equiv 0. \quad (40)$$

The $\mathcal{O}(e^{-c/\epsilon_1})$ remainder term in the $z_{1,a}$ -component is also a $C(\epsilon_1^0(r_1, y_{1,a}, \mu)^k)$ -function with the order being unchanged upon differentiation up to order k with respect to $(r_1, y_{1,a}, \mu)$ for $(\epsilon_1, r_1, y_{1,a}) \in V_{1,a}(\chi)$.

Proof. Since $(\epsilon_1, r_1, y_{1,a})$ -decouples, we use Proposition 3.3 with τ defined by $\epsilon_{11} = e^\tau \epsilon_1$. Let

$$y_{1,a} = \underline{y}_{1,a}(0, \tau, \epsilon_{11}, r_1, y_{11}, \mu) = e^{-\lambda(\mu)\tau}[y_{11} + \phi(0, \tau, \epsilon_{11}, r_1, y_{11}, \mu)]. \quad (41)$$

The $y_{1,a}$ -component of the transition map is then defined implicitly by this equation as $y_{1,a} \mapsto y_{11}$. Consider therefore $F(u_0, \tau, y_{11}, \mu) = 0$ with

$$F(u_0, \tau, r_1, y_{11}, \mu) := u_0 - (y_{11} + \phi(0, \tau, \epsilon_{11}, r_1, y_{11}, \mu)),$$

for $\epsilon_{11} > 0$ fixed, defined by setting the square bracket in (41) equal to u_0 . Then by Proposition 3.3 and the implicit function theorem, we obtain a locally unique solution

$$y_{11} = u_0 + \tilde{\psi}_{1,a}(\tau, r_1, u_0, \mu), \quad (42)$$

of $F = 0$ with $\tilde{\psi}_{1,a} \in C^k$ for all $\tau > 0$ large enough and $0 \leq |u|, r_1, \epsilon_{11}, |\mu| \leq \chi$. With $\epsilon_{11} > 0$ fixed in the following we suppress its dependency from $\tilde{\psi}_{1,a}$. Inserting $u_0 = e^{\lambda(\mu)\tau} y_{1,a} = (\epsilon_{11} \epsilon_1^{-1})^{\lambda(\mu)} y_{1,a}$ into the right hand side of (42) and defining

$$\psi_{1,a}(\epsilon_1, r_1, u_0, \mu) := \tilde{\psi}_{1,a}(\log(\epsilon_1^{-1} \epsilon_{11}), r_1, u_0, \mu)$$

give the desired expression for the $y_{1,a}$ -component of $P_{1,a}$ on the set $V_{1,a}(\chi)$. The function $\psi_{1,a}$ extends to a $C((\epsilon_1^0(r_1, u_0, \mu))^k)$ -function on the closed interval $\epsilon_1 \in [0, \epsilon_{10}]$ due to the Arzela-Ascoli theorem, Proposition 3.3 (with $k \rightarrow k + 1$) and the uniform boundedness of ϕ in C^{k+1} . The bound in $C((\epsilon_1, r_1)^0(r_1, u_0, \mu)^k)$ in (40) follows from (38). Finally, the equality in (40) follows from the invariance of $r_1 = y_{1,a} = 0$ for (37) (due to the existence of (12)), see also the second equality in (38).

We subsequently use the transition time $\tau = \log(\epsilon_1^{-1}\epsilon_{11})$ to exponentially estimate the $z_{1,a}$ -component of $P_{1,a}$. This is standard and can be done in C^k with respect to $(r_1, y_{1,a}, \mu)$ through variational equations. This completes the proof. \square

We can do precisely the same thing for $P_{1,r}$ by working in backward time. We therefore state the following results without proof.

Lemma 3.5. *Consider (28) near $M_{1,r}$. Then for $\sigma > 0$ small enough, there exists a regular transformation of time and a smooth diffeomorphism $(y_1, z_1) \mapsto (y_{1,r}, z_{1,r})$, $y_1, z_1 - 1 \in [-\sigma, \sigma]$, depending smoothly on (ϵ_1, r_1, μ) for $0 \leq r_1, \epsilon_1, |\mu| \leq \sigma$, such that*

$$\begin{aligned} y_{1,r} &= h_{1,r}^0(\epsilon_1, r_1, y_1, \mu) + \epsilon_1 h_{1,r}^1(\epsilon_1, r_1, y_1, z_1, \mu), \\ z_{1,r} &= z_1 - m_{1,r}(\epsilon_1, r_1, y_1, \mu), \end{aligned} \quad (43)$$

where

$$h_{1,r}^0(\epsilon_1, 0, \mu, \mu) \equiv 0, \quad \frac{\partial h_{1,r}^0}{\partial y_1}(\mathbf{0}) = 1, \quad \frac{\partial h_{1,r}^0}{\partial \mu}(\mathbf{0}) = -1, \quad (44)$$

and (28) becomes

$$\begin{aligned} \dot{r}_1 &= \frac{1}{2}r_1\epsilon_1, \\ \dot{y}_{1,r} &= ((-\lambda(\mu) + r_1 L_0(r_1, y_{1,a}, \mu))y_{1,a} + r_1\epsilon_1 L_1(\epsilon_1, r_1, y_{1,a}, \mu))\epsilon_1, \\ \dot{z}_{1,r} &= (2 + L_2(r_1, y_{1,a}, z_{1,a}, \epsilon_1, \mu))z_{1,r}, \\ \dot{\epsilon}_1 &= -\epsilon_1^2, \end{aligned} \quad (45)$$

with L_0, L_1, L_2 each smooth and $L_2(\mathbf{0}) = 0$.

We can as above extend the normal form transformation to $z_1 \in [0, 1 + \sigma]$, say, by the flow-box theorem.

Let $\tilde{m}_{1,r}(\epsilon_1, r_1, y_{1,r}, \mu) = m_{1,r}(r_1, y_1(\epsilon_1, r_1, y_{1,r}, \mu), \epsilon_1, \mu)$ with the smooth function $y_1(\epsilon_1, r_1, y_{1,r}, \mu)$ being obtained (by the implicit function theorem) from (43) with $z_1 = 0$:

$$y_{1,r} = h_{1,r}^0(\epsilon_1, r_1, y_1, \mu) + \epsilon_1 h_{1,r}^1(\epsilon_1, r_1, y_1, 0, \mu).$$

Proposition 3.6. *Fix $k \in \mathbb{N}$ and any $\delta > 0$. Then there exist constants $c > 0$, $\chi > 0$ and $0 < \epsilon_{10} \ll \epsilon_{11}$, $r_{10} > 0$ such that the following holds: The transition map $P_{1,r}(\cdot, \mu)$ of (45) from $\{z_{1,r} = -\tilde{m}_{1,r}(\epsilon_1, r_1, y_{1,r}, \mu)\}$ to $\{\epsilon_1 = \epsilon_{11}\}$ is well-defined on a region $V_{1,r}(\chi)$ defined by*

$$|y_{1,r}| \leq \chi(\epsilon_1\epsilon_{11}^{-1})^{\lambda(\mu)}, \quad \epsilon_1 \in [0, \epsilon_{10}], \quad r_1 \in [0, r_{10}], \quad (46)$$

and on this region, the mapping takes the following form

$$P_{1,r}(\epsilon_1, r_1, y_{1,r}, \mu) = \begin{pmatrix} \sqrt{\epsilon_1 \epsilon_{11}^{-1}} r_1 \\ (\epsilon_{11} \epsilon_1^{-1})^{\lambda(\mu)} y_{1,r} + \psi_{1,r}(\epsilon_1, r_1, (\epsilon_1^{-1} \epsilon_{11})^{\lambda(\mu)} y_{1,a}, \mu) \\ \mathcal{O}(e^{-c/\epsilon_1}) \\ \epsilon_{11} \end{pmatrix}.$$

Here $\psi_{1,r}$ is a $C((\epsilon_1^0(r_1, u, \mu))^k)$ -function on the set $r_1 \in [0, r_{10}]$, $\epsilon_1 \in [0, \epsilon_{10}]$, $0 \leq |u|, |\mu| \leq \chi$ with

$$\|\psi_{1,r}\|_{(\epsilon_1, r_1)^0(u, \mu)^k} \leq \delta, \quad \psi_{1,r}(\epsilon_1, 0, 0, \mu) \equiv 0. \quad (47)$$

The $\mathcal{O}(e^{-c/\epsilon_1})$ remainder term in the $z_{1,r}$ -component is also a $C((\epsilon_1, r_1)^0(y_{1,r}, \mu)^k)$ -function with the order being unchanged upon differentiation up to order k with respect to $(y_{1,r}, \mu)$ in $V_{1,r}(\chi)$.

Remark 3.7. Notice that if we define $\hat{y}_{1,a}$ and $\hat{y}_{1,r}$ by

$$y_{1,i} = (\epsilon_1 \epsilon_{11}^{-1})^{\lambda(\mu)} \hat{y}_{1,i}, \quad i = a, r \quad (48)$$

for $\epsilon_1 \in (0, \epsilon_{10}]$ then $V_{1,i}$ and $V_{1,r}$ are “blown up” to $\hat{y}_{1,i} \in [-\chi, \chi]$, $i = a, r$, and the $y_{1,i}$ -components of $P_{1,i}$

$$\hat{y}_{1,i} + \psi_{1,i}(r_1, \epsilon_1, \hat{y}_{1,i}, \mu),$$

become regular as functions of $(r_1, \hat{y}_{1,i}, \mu)$ for $i = a, r$. We will use a similar – but slightly different scaling – later on. The reason why (48) will not work directly, is that we also have to transform μ appropriately in order to relate $y_{1,a}$ and $y_{1,r}$ (through their relationship to y_1) in such a way that the application of $P_{1,a}$ and $P_{1,r}$ correspond to flowing the same point forward and backward in time.

3.2 Analysis in the $\bar{\epsilon} = 1$ -chart

Having now followed points on $\{z_1 = 0\}$ forwards and backwards until the section $\{\epsilon_1 = \epsilon_{11}\}$, we proceed to extend these further into the scaling chart. Here the equations are given by (9). Notice specifically that $\epsilon_1 = \epsilon_{11} > 0$ in the $\bar{x} = -1$ -chart corresponds to $x_2 = -\epsilon_{11}^{-1}$ in the scaling chart.

Let $P_{2,a}$ and $P_{2,r}$ denote the mappings from $\{x_2 = -\epsilon_{11}^{-1}\}$ to $\{z_2 = 0\}$ near $\gamma_{2,0}(0)$, obtained by the first intersection upon application of the forward respectively backward flow of (9). Each of these mappings are regular, i.e. smooth diffeomorphisms.

Through the flow of (9) we can also extend the center manifolds $M_{2,a}$ and $M_{2,r}$, being the coordinate transformations of $M_{1,a}$ and $M_{1,r}$, respectively, using (8). The manifolds $M_{2,a}$ and $M_{2,r}$ within the (x_2, y_2, z_2, r_2) -space are foliated by constant values of $r_2 \sim 0$. Let $M_{2,a}(r_2)$ and $M_{2,r}(r_2)$ denote the corresponding leaves of this foliation projecting onto the (x_2, y_2, z_2) -space. It is standard, see [39], that $M_{2,a}(0)$ and $M_{2,r}(0)$ intersect transversally along $\gamma_{2,0}(\mu)$ for all $\mu \sim 0$. This gives rise to a connecting orbit $\gamma_{2,r_2}(\mu) = M_{2,a}(r_2) \cap M_{2,r}(r_2)$ for all $0 < r_2 = \sqrt{\bar{\epsilon}} \ll 1$, see [39]. In this way, one may obtain the perturbed (maximal) strong canard $\gamma_\epsilon(\mu)$ with $\lim_{\epsilon \rightarrow 0} \gamma_\epsilon(\mu) \rightarrow \gamma_0(\mu)$, see [39].

3.3 Putting it all together

We summarize the local findings in charts into a global diagram in Fig. 4. Notice that the strong canard orbit γ_0 (in orange) is a heteroclinic orbit of partially hyperbolic points on the blowup sphere. For $\mu = 0$, there is a fast jump (in black) that together with γ_0 gives rise to heteroclinic cycle. It is the perturbation of this cycle, that produce the intermediate periodic orbits that connect to the small ones (as perturbations of the green orbits, recall Fig. 2) and canard cycles.

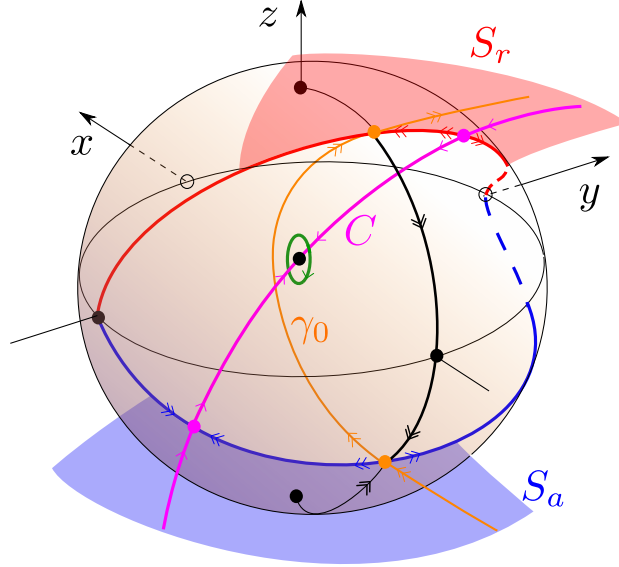


Figure 4: Dynamics for the blown up system for $\mu = 0$.

We now define $\Delta_a(\epsilon_1, r_1, y_{1,a}, \mu)$ in the following way:

$$\Delta_a(\epsilon_1, r_1, y_{1,a}, \mu) = \left(\Pi \circ P_{2,a} \circ \widehat{C}_{21} \circ P_{1,a} \right) (\epsilon_1, r_1, y_{1,a}, \mu),$$

with Π the projection onto the (x_2, y_2) -plane and where \widehat{C}_{21} is the change of coordinates from $(\epsilon_1, r_1, y_{1,a}, z_{1,a})$ to (x_2, y_2, z_2, r_2) defined by (33) and (8). Δ_a therefore describes the transition map from $\{z_1 = 0\}$ in chart $\bar{x} = -1$, using the coordinates $(\epsilon_1, r_1, y_{1,a})$, to $\{z_2 = 0\}$ in chart $\bar{x} = 1$, using the coordinates (x_2, y_2) for $r_2 = \sqrt{\epsilon} = r_1 \sqrt{\epsilon_1}$. We define Δ_r completely analogously:

$$\Delta_r(\epsilon_1, r_1, y_{1,r}, \mu) = \left(\Pi \circ P_{2,r} \circ \widehat{C}_{21} \circ P_{1,r} \right) (\epsilon_1, r_1, y_{1,r}, \mu).$$

If $(\epsilon_1, r_1, y_{1,a}) \in V_{1,a}(\chi)$ and $(\epsilon_1, r_1, y_{1,r}) \in V_{1,r}(\chi)$, under the coordinate transformations (33) and (43) for $z_1 = 0$, correspond to the same point $(\epsilon_1, r_1, y_1, 0)$ on the section $\{z_1 = 0\}$ in the $\bar{x} = -1$ -chart, then $\Delta_a(\epsilon_1, r_1, y_{1,a}, \mu) = \Delta_r(\epsilon_1, r_1, y_{1,r}, \mu)$ for $r_1 \geq 0$, $\epsilon_1 > 0$ clearly implies existence of a closed orbit of $((3), \dot{\epsilon} = 0)$ system through the point given by $(\epsilon_1, r_1, y_1, 0) \in \{z_1 = 0\}$ in the $\bar{x} = -1$ -chart.

Solving (33) and (43) with $z_1 = 0$ for y_1 , we find that

$$y_1 = \bar{h}_{1,a}(\epsilon_1, r_1, y_{1,a}, \mu),$$

and

$$y_1 = \bar{h}_{1,r}(\epsilon_1, r_1, y_{1,r}, \mu),$$

by applying the inverse/implicit function theorem. Here $\bar{h}_{1,i}$ have the same smoothness properties as $h_{1,i}$, $\bar{h}_{1,i}(\epsilon_1, \mathbf{0}) \equiv 0$, $i = a, r$, and

$$\frac{\partial \bar{h}_{1,a}}{\partial y_{1,a}}(\mathbf{0}) = 1, \quad \frac{\partial \bar{h}_{1,a}}{\partial \mu}(\mathbf{0}) = -1, \quad (49)$$

$$\frac{\partial \bar{h}_{1,r}}{\partial y_{1,r}}(\mathbf{0}) = 1, \quad \frac{\partial \bar{h}_{1,r}}{\partial \mu}(\mathbf{0}) = 1. \quad (50)$$

Equating these expressions for y_1 , we obtain the following equation

$$L(\epsilon_1, r_1, y_{1,a}, y_{1,r}, \mu) := \bar{h}_{1,a}(\epsilon_1, r_1, y_{1,a}, \mu) - \bar{h}_{1,r}(\epsilon_1, r_1, y_{1,r}, \mu) = 0, \quad (51)$$

relating $y_{1,a}$ and $y_{1,r}$, as desired. We can use the implicit function theorem to solve this equation for $y_{1,r}$ as function of $(\epsilon_1, r_1, y_{1,a}, \mu)$. Subsequently, since we are interested in applying both $P_{1,a}$ and $P_{1,r}$, we need to ensure that the image of the region $V_{1,a}(\chi)$ (or an appropriate subset hereof) under the associated mapping $(\epsilon_1, r_1, y_{1,a}) \mapsto (\epsilon_1, r_1, y_{1,r})$ defined by (51), will be contained within $V_{1,r}(\chi)$. For this, we therefore first adjust μ .

Lemma 3.8. *There exists a continuous function $\mu_0(\epsilon_1, r_1)$ with $\mu_0(\epsilon_1, 0) \equiv 0$ such that $L(\epsilon_1, r_1, 0, 0, \mu_0(\epsilon_1, r_1)) = 0$ for all $\epsilon_1 \in [0, \epsilon_{10}]$, $r_1 \in [0, r_{10}]$.*

Proof. Simple application of the implicit function theorem using $L(\epsilon_1, \mathbf{0}) = 0$ and $L'_\mu(\mathbf{0}) = -2$. \square

Remark 3.9. *Clearly, $\mu_0 \in C(\epsilon_0^0 r_1^k)$ but we will not use the smoothness in r_1 in the proof Theorem 1.1. This relates to the fact that the statement is only that $\bar{\mu}(h, \epsilon)$ is continuous. In the author's opinion, the smoothness properties of this function with respect to h is more involved and certainly more difficult to state. The interpretation of μ_0 within $\epsilon_1 = 0$ is illustrated in Fig. 3(b).*

Following on from this, we then obtain:

Lemma 3.10. *The equation*

$$L(\epsilon_1, r_1, y_{1,a}, y_{1,r}, \mu_0(\epsilon_1, r_1) + \tilde{\mu}) = 0,$$

has a locally unique solution of the form

$$y_{1,r} = h_{ra}(\epsilon_1, r_1, y_{1,a}, \tilde{\mu}), \quad (52)$$

with $h_{ra} \in C((\epsilon_1, r_1)^0 (y_{1,a}, \tilde{\mu})^k)$ and

$$h_{ra}(\epsilon_1, r_1, 0, 0) \equiv 0, \quad \frac{\partial h_{ra}}{\partial y_{1,a}}(\mathbf{0}) = 1, \quad \frac{\partial h_{ra}}{\partial \tilde{\mu}}(\mathbf{0}) = -2. \quad (53)$$

Proof. Follows from the implicit function theorem, using

$$L(\epsilon_1, r_1, 0, 0, \mu_0(\epsilon_1, r_2)) = 0, \quad L'_{y_{1,r}}(\epsilon_1, r_1, 0, 0, \mu_0(\epsilon_1, r_1)) \approx 1.$$

\square

Due to (53) and the mean value theorem, $h_{ra}(\epsilon_1, r_1, y_{1,a}, \tilde{\mu}) = y_{1,a}(\cdots) + \tilde{\mu}(\cdots)$ which leads to the following.

Lemma 3.11. *Let $\sigma > 0$, $0 < \chi_i < \chi$ for $i = a, r$. Define the scaled quantities $\hat{y}_{1,a}, \hat{y}_{1,r}, \hat{\mu}$ by*

$$y_{1,a} = (\epsilon_1 \epsilon_{11}^{-1})^{\lambda(\mu_0)} \hat{y}_{1,a}, \quad y_{1,r} = (\epsilon_1 \epsilon_{11}^{-1})^{\lambda(\mu_0)} \hat{y}_{1,r}, \quad \mu = \mu_0(\epsilon_1, r_1) + (\epsilon_1 \epsilon_{11}^{-1})^{\lambda(\mu_0)} \hat{\mu}, \quad (54)$$

for $\epsilon_1 > 0$. Then we have the following.

1. For $\epsilon_{10} > 0$ small enough, with $y_{1,i}$ given by (54) for

$$\hat{y}_{1,a} \in [-\chi_a, \chi_a], \quad \hat{y}_{1,r} \in [-\chi_r, \chi_r], \quad \hat{\mu} \in [-\sigma, \sigma], \quad (55)$$

we have $(\epsilon_1, r_1, y_{1,i}) \in V_{1,i}(\chi)$, $i = a, r$ for all $\epsilon_1 \in (0, \epsilon_{10}]$.

2. (52) becomes

$$\hat{y}_{1,r} = \hat{h}_{ra}(\epsilon_1, r_1, \hat{y}_{1,a}, \hat{\mu}) := (\epsilon_1 \epsilon_{11}^{-1})^{-\lambda(\mu_0)} h_{ra}(\epsilon_1, r_1, (\epsilon_1 \epsilon_{11}^{-1})^{\lambda(\mu_0)} \hat{y}_{1,a}, (\epsilon_1 \epsilon_{11}^{-1})^{\lambda(\mu_0)} \hat{\mu}),$$

for $\epsilon_1 \in (0, \epsilon_{10}]$. \hat{h}_{ra} has a $C((\epsilon_1, r_1)^0 (\hat{y}_{1,a}, \hat{\mu})^{k-1})$ -extension to the closed interval $\epsilon_1 \in [0, \epsilon_{10}]$ with $\hat{h}_{ra}(\epsilon_1, r_1, 0, 0) \equiv 0$.

3. $\hat{h}_{ra}(0, r_1, \cdot, \cdot)$ is linear and for $r_1 = 0$:

$$\hat{h}_{ra}(0, 0, \hat{y}_{1,a}, \hat{\mu}) = \hat{y}_{1,a} - 2\hat{\mu}.$$

4. For $\sigma > 0$, $r_{10} > 0$ and $\epsilon_{10} > 0$ all small enough, we have that:

$$\hat{h}_{ra}(\epsilon_1, r_1, \hat{y}_{1,a}, \hat{\mu}) \in (-\chi, \chi),$$

for all $\epsilon_1 \in [0, \epsilon_{10}]$, $r_1 \in [0, r_{10}]$, $\hat{y}_{1,a} \in [-\chi_a, \chi_a]$, $\hat{\mu} \in [-\sigma, \sigma]$.

Proof. Recall from (39) and (46) that $(\epsilon_1, r_1, y_{1,i}) \in V_{1,i}(\chi)$ with $\epsilon_1 > 0$ if and only if

$$(\epsilon_1^{-1} \epsilon_{11})^{\lambda(\mu)} |y_{1,i}| \leq \chi. \quad (56)$$

Now, by (32) and (54) for $|\hat{y}_{1,i}| \leq \chi_i$ the left hand side of (56) becomes

$$(\epsilon_1 \epsilon_{11}^{-1})^{(\epsilon_1 \epsilon_{11}^{-1})^{\lambda(\mu_0(\epsilon_1, r_1))} \hat{\mu}} |\hat{y}_{1,i}| \leq e^{(\epsilon_1 \epsilon_{11}^{-1})^{\lambda(\mu_0(\epsilon_1, r_1))} \hat{\mu} \log(\epsilon_1 \epsilon_{11}^{-1})} \chi_i = (1 + \mathcal{O}(\epsilon_1^{\lambda(\mu_0)} \log \epsilon_1)) \chi_i, \quad (57)$$

and the item 1 therefore follows. Items 2 and 3 follow from Lemma 3.10; notice we lose one degree of smoothness due to the application of the mean value theorem. Finally, item 4 follows from 2 and 3 using $0 < \chi_a < \chi$ and $\epsilon_{10} > 0$ small enough. \square

The implications of item 1. are the following: Let

$$\hat{P}_{1,i}(\epsilon_1, r_1, \hat{y}_{1,a}, \hat{\mu}) := P_{1,i}(\epsilon_1, r_1, y_{1,a}, \mu), \quad (58)$$

for $i = a, r$ and with $y_{1,a}$, $y_{1,r}$ and μ on the right hand side given by the expressions in (54). Then we have:

Lemma 3.12. *Fix $\delta > 0$ small enough. Then for $r_{10} > 0$, $\epsilon_{10} > 0$ sufficiently small,*

$$\hat{P}_{1,i} \in C((\epsilon_1, r_1)^0 (\hat{y}_{1,a}, \hat{\mu})^k),$$

$i = a, r$, defined for $\hat{y}_{1,a} \in [-\chi_a, \chi_r]$, $\hat{y}_{1,r} \in [-\chi_r, \chi_r]$, $\hat{\mu} \in [-\sigma, \sigma]$, $r_1 \in [0, r_{10}]$, $\epsilon_1 \in [0, \epsilon_{10}]$. In particular, the $y_{1,i}$ component of $\hat{P}_{1,i}$ takes the following form:

$$\hat{y}_{1,i} + \hat{\psi}_{1,i}(\epsilon_1, r_1, \hat{y}_{1,i}, \hat{\mu}), \quad (59)$$

where

$$\|\hat{\psi}_{1,i}\|_{(\epsilon_1, r_1)^0 (\hat{y}_{1,i}, \hat{\mu})^k} \leq \delta, \quad \hat{\psi}_{1,i}(\epsilon_1, 0, 0, \hat{\mu}) \equiv 0. \quad (60)$$

Proof. We insert (54) into the $y_{1,i}$ -component of $P_{1,i}$. Proceeding as in (57) for the expansion in ϵ_1 we obtain (59). (60) follows from (40) and (47). \square

Moreover, by item 4. we have that the composed mapping

$$(\epsilon_1, r_1, \hat{y}_{1,a}, \hat{\mu}) \mapsto \widehat{P}_{1,r}(\epsilon_1, r_1, \hat{h}_{ra}(\epsilon_1, r_1, \hat{y}_{1,a}, \hat{\mu}), \hat{\mu}), \quad (61)$$

is a $C((\epsilon_1, r_1)^0(\hat{y}_{1,a}, \hat{\mu})^{k-1})$ -function defined for $y_{1,a} \in [-\chi_a, \chi_a]$ and $\hat{\mu} \in [-\sigma, \sigma]$ and all $r_1 \in [0, r_{10}]$, $\epsilon_1 \in [0, \epsilon_{10}]$ for $\sigma > 0$ and $\epsilon_{10} > 0$ small enough.

We now return to the problem of solving $\Delta_a = \Delta_r$ for closed orbits. Define

$$\widehat{\Delta}_i(\epsilon_1, r_1, \hat{y}_{1,i}, \hat{\mu}) = \Delta_i(\epsilon_1, r_1, y_{1,i}, \mu), \quad i = a, r$$

with $y_{1,i}$ and μ on the right hand side given by the expressions (54). By the properties of $\widehat{P}_{1,i}$ and the regularity of C_{21} and $P_{2,i}$, we have $\widehat{\Delta}_i \in C((\epsilon_1, r_1)^0(\hat{y}_{1,i}, \hat{\mu})^k)$ for $i = a, r$. Finally, let

$$\widehat{\Delta}(r_1, \hat{y}_{1,a}, \epsilon_1, \hat{\mu}) := \widehat{\Delta}_r(\epsilon_1, r_1, \hat{h}_{ra}(\epsilon_1, r_1, \hat{y}_{1,a}, \hat{\mu}), \hat{\mu}) - \widehat{\Delta}_a(\epsilon_1, r_1, \hat{y}_{1,a}, \hat{\mu}), \quad (62)$$

for $r_1 \in [0, r_{10}]$, $\hat{y}_{1,a} \in [-\chi_a, \chi_a]$, $\epsilon_1 \in [0, \epsilon_{10}]$, $\hat{\mu} \in [-\sigma, \sigma]$. By Lemma 3.11 item 2, we finally have that $\widehat{\Delta} \in C((\epsilon_1, r_1)^0(\hat{y}_{1,a}, \hat{\mu})^{k-1})$.

Clearly,

$$\widehat{\Delta}(\epsilon_1, r_1, \hat{y}_{1,a}, \hat{\mu}) = \mathbf{0}, \quad (63)$$

defines closed orbits for $\epsilon_1 > 0$, $r_1 \geq 0$ sufficiently small. We therefore proceed to solve this equation. We will do so by solving for $\hat{y}_{1,a}$, $\hat{\mu}$ as functions of ϵ_1 and r_1 using the implicit function theorem. Henceforth we therefore take $k \geq 2$.

Lemma 3.13.

$$\widehat{\Delta}(\mathbf{0}) = \mathbf{0}. \quad (64)$$

Moreover, there exists two nonzero tangent vectors

$$v_i = (*, *, 0) \in T_{\gamma_{2,0}(0) \cap \{z_2=0\}} M_{2,i}(0),$$

$i = a, r$, such that:

$$\begin{aligned} \frac{\partial \widehat{\Delta}}{\partial \hat{y}_{1,a}}(\mathbf{0}) &= \Pi v_r - \Pi v_a, \\ \frac{\partial \widehat{\Delta}}{\partial \hat{\mu}}(\mathbf{0}) &= -2\Pi v_r. \end{aligned} \quad (65)$$

Proof. First, (64) follows from the connection $\gamma_{2,0}(0)$. Next, for the proof of the the partial derivatives, we first focus on the partial derivatives of $\widehat{\Delta}_a$. For this we differentiate $\widehat{P}_{1,a}$. Following Lemma 3.12, see (60), we have $\frac{\partial \widehat{P}_{1,a}}{\partial \hat{\mu}}(\mathbf{0}) = \mathbf{0}$, and hence $\frac{\partial \widehat{\Delta}_a}{\partial \hat{\mu}}(\mathbf{0}) = \mathbf{0}$. Next, by (59)

$$\frac{\partial \widehat{P}_{1,a}}{\partial \hat{y}_{1,a}}(\mathbf{0}) = \begin{pmatrix} 0 \\ 0 \\ 1 + \mathcal{O}(\delta) \\ 0 \end{pmatrix}. \quad (66)$$

Since $\widehat{P}_{1,a}(\mathbf{0}) = (\epsilon_{11}, 0, 0, 0) \in M_{1,a}$, the vector (66) gives a tangent vector to $M_{2,a}(0)$ at $x_2 = -\epsilon_{11}^{-1}$ upon application of the tangent map $T_{(\epsilon_{11},0,0,0)}\widehat{C}_{21}$ of the change of coordinates \widehat{C}_{21} . Consequently, by applying $TP_{2,a}$ we have

$$\frac{\partial \widehat{\Delta}_a}{\partial \hat{y}_{1,a}}(\mathbf{0}) = \Pi v_a,$$

for some nonzero tangent vector $v_a \in T_{\gamma_{2,0}(0) \cap \{z_2=0\}} M_{2,a}(0)$.

$\widehat{\Delta}_r$ can be handled similarly:

$$\frac{\partial \widehat{\Delta}_r}{\partial \hat{y}_{1,r}}(\mathbf{0}) = \Pi v_r, \quad \frac{\partial \widehat{\Delta}_r}{\partial \hat{\mu}}(\mathbf{0}) = \mathbf{0}$$

for some nonzero tangent vector $v_r \in T_{\gamma_{2,0}(0) \cap \{z_2=0\}} M_{2,r}(0)$. The partial derivative (65) with respect to $\hat{\mu}$ then follows from Lemma 3.11, see item 3, and the chain rule. \square

Since the intersection of $M_{a,2}(0)$ and $M_{r,2}(0)$ is transverse along γ_2 , the vectors $v_i, i = a, r$, as well as $\Pi v_i, i = a, r$, are linearly independent and consequently,

$$\det \left(\frac{\partial \widehat{\Delta}}{\partial (\hat{y}_{1,a}, \hat{\mu})}(\mathbf{0}) \right) = \det \begin{pmatrix} \Pi v_r & -\Pi v_a & -2\Pi v_r \end{pmatrix} = 2 \det \begin{pmatrix} \Pi v_a & \Pi v_r \end{pmatrix} \neq 0.$$

In this way, by the implicit function theorem we can solve $\widehat{\Delta}(\epsilon_1, r_1, \hat{y}_{1,a}, \hat{\mu}) = 0$ locally for $(\hat{y}_{1,a}, \hat{\mu})$ as continuous functions of (ϵ_1, r_1) . In this way, we conclude the following.

Proposition 3.14. *There exist continuous functions $\bar{y}(\epsilon_1, r_1), \bar{\mu}(\epsilon_1, r_1), \epsilon_1 \in [0, \epsilon_{10}], r_1 \in [0, r_{10}]$ for $\epsilon_{10} > 0$ and $r_{10} > 0$ small enough, with $\bar{y}(0, 0) = \bar{\mu}(0, 0) = 0$ such that there is a periodic orbit of $((3), \dot{\epsilon} = 0)$ through any point $(\epsilon_1, r_1, \bar{y}(\epsilon_1, r_1), 0)$ in chart $\bar{x} = -1$ for $\mu = \bar{\mu}(\epsilon_1, r_1)$ for all $\epsilon_1 \in (0, \epsilon_{10}], r_1 \in [0, r_{10}]$.*

Proof. After having solved $\widehat{\Delta} = 0$ for $\hat{y}_{1,a}$ and $\hat{\mu}$ as continuous functions (ϵ_1, r_1) by the implicit function theorem using Lemma 3.13, we complete the result by mapping the solution back to the (y_1, μ) -variables. \square

4 Completing the proof of Theorem 1.1

To complete the proof of Theorem 1.1, we first collect our results thus far: First, by Proposition 2.11 we have for any $h_1 > 0$ a family of periodic orbits $\Gamma_{2,h,\epsilon}^{\text{small}}, h \in (0, h_1]$, of (9) with $\mu = r_2 \bar{\mu}_2(h, \epsilon)$ for all $r_2 = \sqrt{\epsilon} > 0$ small enough, parametrized in the \tilde{u} -variables, see (21), by their intersection $\tilde{u} = (-h, 0), y_2 = \bar{y}_2(h, r_2)$ with $\tilde{u}_2 = 0$.

Lemma 4.1. *Consider (9) for parameter values $\mu \in [-\delta, \delta]$, and let D be any compact domain in the phase (x_2, z_2) -plane. Then there is an $h_1 > 0$ such that any periodic orbit of this system for $r_2 > 0$ small enough, that is contained within the set defined by $(x_2, z_2) \in D, y_2 \in [-\delta, \delta]$ and intersects $\tilde{u}_1 < 0, \tilde{u}_2 = 0$ in a single point, belongs to the family $\Gamma_{2,h,\epsilon}^{\text{small}}, h \in (0, h_1]$.*

Proof. The statement is clearly true for $\mu = r_2 \mu_2$ with $\mu_2 \in [-\delta, \delta]$ for $\delta > 0$ small enough, since the family $\Gamma_{2,h,r_2}, h \in (0, h_1]$, is obtained by the implicit function theorem. Next, we realize that there are no periodic orbits for any $|\mu_2| > \delta$ and $r_2 > 0$ small enough since in this case, the equilibrium (14) is hyperbolic; specifically, C_2 is normally hyperbolic in a neighborhood of (14). Finally, for $r_2 c \leq |\mu| \leq \delta$ with $c > 0$ large enough, y_2 has a single sign in the set $(x_2, z_2) \in D, y_2 \in [-\delta, \delta]$, completing the proof. \square

Clearly, the family $\Gamma_{2,h,\epsilon}^{\text{small}}$, $h \in (0, h_1]$, becomes a family of “small” periodic orbits $\Gamma_{h,\epsilon}^{\text{small}}$ of (3) upon blowing down, intersecting $z = 0$ in $x \sim \sqrt{\epsilon}h$, $y = r_2\bar{y}_2(h, \sqrt{\epsilon})$, $h \in (0, h_1]$. (Here we have used \sim in the expression for x since this only holds to leading order; the family is parametrized by $\tilde{u}_1 = h$ and x_2 and \tilde{u}_1 differ by $\mathcal{O}(\sqrt{\epsilon})$ in the relevant domain.)

Remark 4.2. *As documented in [21], there may exist bifurcations along Γ_{2,h,r_2} (periodic doubling- and torus bifurcations). This does not contradict Lemma 4.1, since this lemma only addresses the uniqueness of the branch of periodic orbits intersecting $u_1 < 0$ once.*

Next, we turn to the intermediate periodic orbits obtained from Proposition 3.14. Here we obtain a family of periodic orbits $\Gamma_{h,\epsilon}^{\text{inter}}$, $h \in [\sqrt{\epsilon}/\sqrt{\epsilon_{11}}, r_{10}]$, of (3) with $\mu = \bar{\mu}(h^{-2}\epsilon, h)$ for all $\epsilon > 0$ small enough, parametrized by their intersecting $(x, z) = (-h, 0)$ and $y = h\bar{y}(h^{-2}\epsilon, h)$. This follows from Proposition 3.14 and (6), specifically $\epsilon = r_1^2\epsilon_1$ and $r_1 = h$. Now, $r_1 = h = \sqrt{\epsilon}/\sqrt{\epsilon_{11}}$ corresponds to $\epsilon_1 = \epsilon_{11}$ or $x_2 = -1/\epsilon_{11}$ upon change of coordinates (8). Consequently, upon taking $h_1 > -1/\sqrt{\epsilon_{11}}$ the branch $\Gamma_{2,h,\epsilon}^{\text{inter}}$, i.e. $\Gamma_{h,\epsilon}^{\text{inter}}$ written in the coordinates of the $\bar{\epsilon} = 1$ -chart, overlap with $\Gamma_{2,h,\epsilon}^{\text{small}}$ for all $0 < \epsilon \ll 1$. By Lemma 4.1, where they overlap, they coincide for all $0 < \epsilon \ll 1$. In this way, we obtain the desired family by gluing the two branches together in the domain where they overlap.

5 Discussion

Our main theorem generalizes the birth of canard cycles in \mathbb{R}^2 , see e.g. [33], to \mathbb{R}^3 through the folded saddle-node of type II and the strong canard. In contrast to the result in [33], our results are – however – only local. Nevertheless, it is also possible to use our method to obtain more global results. We have illustrated a situation in Fig. 5(a). Here we can also follow the forward and backward flow of the set of points on the section (in orange) that is indicated in the figure using the normal forms and the solutions of the Shilnikov problem, see Lemma 3.2 and Proposition 3.3. In contrast to $P_{2,i}, i = a, r$, above, we would just define transition maps from $r_1 = r_{10}$ fixed to $\epsilon_1 = \epsilon_{11}$. Otherwise, the proof for the existence of closed orbits, would proceed analogously, using that the center manifolds $M_{a,r}$ intersect transversally along the strong canard $\gamma_0(\mu)$. The same holds for the perturbation of the singular cycles in Fig. 5(b) (however, the transition from (a) to (b) is more complicated). These extensions could even be done in the smooth setting. The cycles in Fig. 5(c) mark the end of canard cycles and in \mathbb{R}^2 this is where classical relaxation oscillations appear. However, in contrast to \mathbb{R}^2 the folded singularity p can be of different types, e.g. folded nodes or folded saddles. In future work, we will describe the transition to relaxation oscillations in \mathbb{R}^3 .

We prove our result in the analytic setting. In particular, we used analyticity to prove existence of a slow manifold, that is not normally hyperbolic but acts as the center of (normal) oscillations. This in connection with Melnikov theory, enabled an extension of the Hopf cycles. Although results on normally elliptic slow manifolds [4, 7, 11, 31] are almost exclusively in the analytic setting, it seems plausible that the result could be extended to the smooth setting, perhaps using (approach (ii), mentioned in the introduction, and) the structure of (9) more explicitly.

Finally, we note that our main result does not rely upon analyticity with respect to ϵ , only in the space variables. This suggests that our results do also apply to systems that have been reduced from higher dimensions. Indeed, slow manifolds in analytic systems have been shown to be analytic in space variables (and only Gevrey-1 smooth in ϵ), see e.g. [11] and references herein.

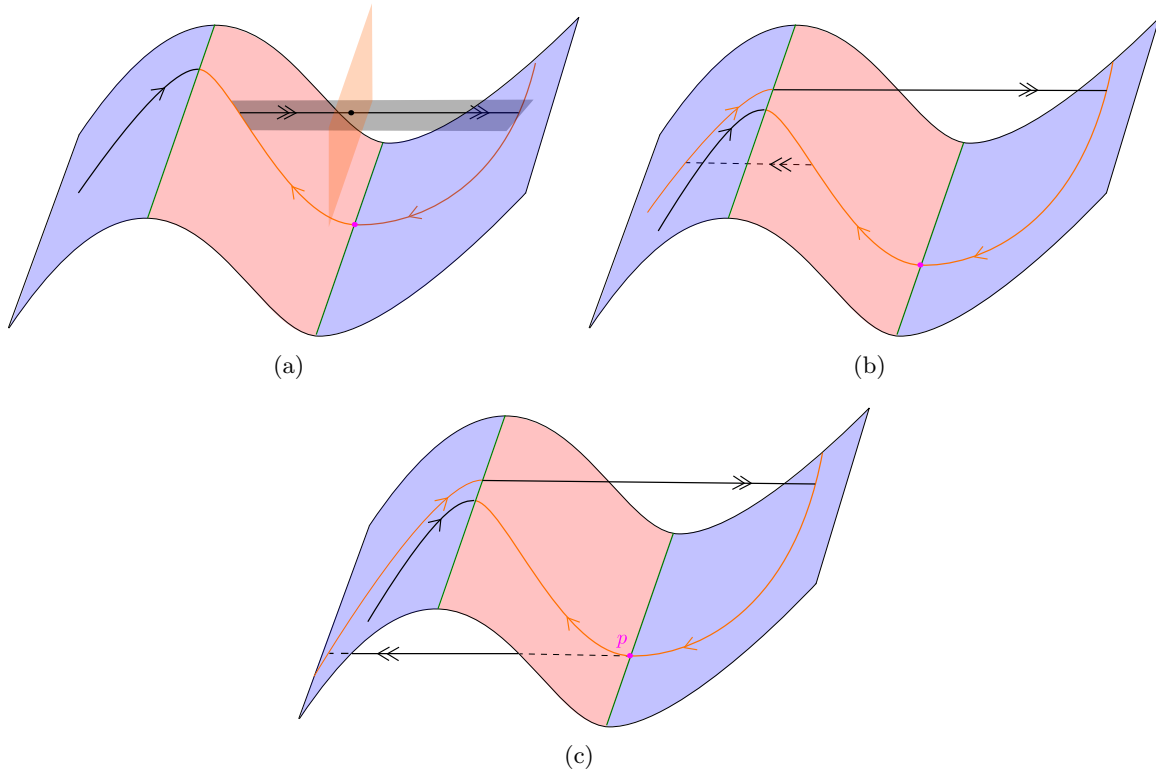


Figure 5: Canard cycles in \mathbb{R}^3 in the case of a S -shaped critical manifold. In (a): canard cycle without head, (b): canard cycles with head and (c): the end of the canard cycles, where transition to classical relaxation oscillations appear.

References

- [1] R. Amir, M. Michaelis, and M. Devor. Burst discharge in primary sensory neurons: triggered by subthreshold oscillations, maintained by depolarizing afterpotentials. *Journal of Neuroscience*, 22(3):1187–1198, 2002.
- [2] I. Baldomá, S. Ibáñez, and T.M. Seara. Hopf-zero singularities truly unfold chaos. *Communications in Nonlinear Science and Numerical Simulation*, 84:105162, 2019.
- [3] I. Baldomá and T. M. Seara. The inner equation for generic analytic unfoldings of the Hopf-zero singularity. *Discrete and Continuous Dynamical Systems - Series B*, 10(2-3):323–347, 2008.
- [4] W. Balser. *From Divergent Power Series to Analytic Functions : Theory and Application of Multisummable Power Series*. Springer, 1994.
- [5] E. Benoit. Singular perturbation, tridimensional case: Canards on a pseudo-singular node point. *Bulletin De La Societe Mathematique De France*, 129(1):91–113, 2001.
- [6] E. Benoit, J. L. Callot, F. Diener, and M. Diener. Chasse au canard. *Collect. Math.*, 31-32:37–119, 1981.
- [7] B.L.J. Braaksma. Multisummability of formal power-series solutions of nonlinear meromorphic differential-equations. *Annales De L Institut Fourier*, 42(3):517–540, 1992.

- [8] H. W. Broer and G. Vegter. Subordinate Šil'nikov bifurcations near some singularities of vector fields having low codimension. *Ergodic Theory and Dynamical Systems*, 4(04), 1984.
- [9] M. Brøns and K. Bar-Eli. Canard explosion and excitation in a model of the Belousov-Zhabotinsky reaction. *Journal of Physical Chemistry*, 95:8706–8713, 1991.
- [10] M. Brøns, M. Krupa, and M. Wechselberger. Mixed mode oscillations due to the generalized canard phenomenon. In W. Nagata and N. Sri Namachchivaya, editors, *Bifurcation Theory and Spatio-Temporal Pattern Formation*, volume 49 of *Fields Institute Communications*, pages 39–64. American Mathematical Society, 2006.
- [11] P. De Maesschalck and K. Kenens. Gevrey asymptotic properties of slow manifolds. *Nonlinearity*, 33(1):341–387, 2020.
- [12] B. Deng. The Shilnikov problem, exponential expansion, strong λ -lemma, C1-linearization, and homoclinic bifurcation. *Journal of Differential Equations*, 79(79):189–231, 1988.
- [13] M. Desroches, J. Guckenheimer, B. Krauskopf, H. M. Osinga, C. Kuehn, and M. Wechselberger. Mixed-mode oscillations with multiple time scales. *SIAM Review*, 54(2):211–288, 2012.
- [14] F. Dumortier, J. Llibre, and J. C. Artés. *Qualitative theory of planar differential systems*. Springer Berlin Heidelberg, 2006.
- [15] F. Dumortier and R. Roussarie. Canard cycles and center manifolds. *Mem. Amer. Math. Soc.*, 121:1–96, 1996.
- [16] I. R. Epstein and K. Showalter. Nonlinear chemical dynamics: Oscillations, patterns, and chaos. *Journal of Physical Chemistry*, 100(31):13132–13147, 1996.
- [17] N. Fenichel. Persistence and smoothness of invariant manifolds for flows. *Indiana University Mathematics Journal*, 21:193–226, 1971.
- [18] N. Fenichel. Asymptotic stability with rate conditions. *Indiana University Mathematics Journal*, 23:1109–1137, 1974.
- [19] N. Fenichel. Geometric singular perturbation theory for ordinary differential equations. *J. Diff. Eq.*, 31:53–98, 1979.
- [20] A. Goryachev, P. Strizhak, and R. Kapral. Slow manifold structure and the emergence of mixed-mode oscillations. *Journal of Chemical Physics*, 107(8):2881–2889, 1997.
- [21] J. Guckenheimer. Singular Hopf bifurcation in systems with two slow variables. *SIAM Journal on Applied Dynamical Systems*, 7(4):1355–1377, 2008.
- [22] J. Guckenheimer and P. Holmes. *Nonlinear Oscillations, Dynamical Systems and Bifurcations of Vector Fields*. Springer Verlag, 5th edition, 1997.
- [23] J. Guckenheimer and I. Lizarraga. Shilnikov homoclinic bifurcation of mixed-mode oscillations. *Siam Journal on Applied Dynamical Systems*, 14(2):764–786, 2015.
- [24] Y.S. Ilyashenko and S.Y. Yakovenko. Finitely-smooth normal forms of local families of diffeomorphisms and vector-fields. *Russian Mathematical Surveys*, 46(1):1–43, 1991.

- [25] E. M. Izhikevich. *Dynamical Systems in Neuroscience: The geometry of Excitability and Bursting*. The MIT Press, 2007.
- [26] C. K. R. T. Jones. *Geometric Singular Perturbation Theory, Lecture Notes in Mathematics, Dynamical Systems (Montecatini Terme)*. Springer, Berlin, 1995.
- [27] A. Kelley. The stable, center-stable, center, center-unstable, unstable manifolds. *Journal of Differential Equations*, 3:546–570, 1967.
- [28] M.T.M. Koper and P. Gaspard. Mixed-mode and chaotic oscillations in a simple-model of an electrochemical oscillator. *Journal of Physical Chemistry*, 95(13):4945–4947, 1991.
- [29] M.T.M. Koper and P. Gaspard. The modeling of mixed-mode and chaotic oscillations in electrochemical systems. *Journal of Chemical Physics*, 96(10):7797–7813, 1992.
- [30] K. U. Kristiansen and M. G. Pedersen. Mixed-mode oscillations in coupled fitzhugh-nagumo oscillators: blowup analysis of cusped singularities, 2022.
- [31] K. U. Kristiansen and C. Wulff. Exponential estimates of symplectic slow manifolds. *Journal of Differential Equations*, 261(1):56–101, 2016.
- [32] M. Krupa and P. Szmolyan. Extending geometric singular perturbation theory to non-hyperbolic points - fold and canard points in two dimensions. *SIAM Journal on Mathematical Analysis*, 33(2):286–314, 2001.
- [33] M. Krupa and P. Szmolyan. Relaxation oscillation and canard explosion. *Journal of Differential Equations*, 174(2):312–368, 2001.
- [34] M. Krupa and M. Wechselberger. Local analysis near a folded saddle-node singularity. *Journal of Differential Equations*, 248(12):2841–2888, 2008.
- [35] C. Kuehn. *Multiple Time Scale Dynamics*. Springer-Verlag, Berlin, 2015.
- [36] T. Matsumoto, R. Tokunaga, M. Komuro, and H. Kokubu. *Bifurcations*. Springer Japan, 1993.
- [37] J. Mujica, B. Krauskopf, and H. M. Osinga. Tangencies between global invariant manifolds and slow manifolds near a singular hopf bifurcation. *SIAM Journal on Applied Dynamical Systems*, 17(2):1395–1431, 2017.
- [38] J. Rinzel. A formal classification of bursting mechanisms in excitable systems. *Mathematical Topics in Population Biology, Morphogenesis and Neurosciences*, pages 267–281, 1987.
- [39] P. Szmolyan and M. Wechselberger. Canards in \mathbb{R}^3 . *J. Diff. Eq.*, 177(2):419–453, December 2001.
- [40] B. van der Pol. A theory of the amplitude of free and forced triode vibrations. *Radio Review*, 1(15):754–762, 1920.
- [41] T. Vo, R. Bertram, and M. Wechselberger. Bifurcations of canard-induced mixed mode oscillations in a pituitary lactotroph model. *Discrete and Continuous Dynamical Systems*, 32(8):2879–2912, 2012.
- [42] T. Vo and M. Wechselberger. Canards of folded saddle-node type i. *SIAM Journal on Applied Dynamical Systems*, 47(4):3235–3283, 2015.

- [43] M. Wechselberger. Existence and bifurcation of canards in \mathbb{R}^3 in the case of a folded node. *SIAM Journal on Applied Dynamical Systems*, 4(1):101–139, January 2005.

A Proof of Proposition 3.3

We write $y_1(t) = e^{\lambda(\mu)(t-\tau)}u(t)$. Then from (37) and variation of constants we have

$$\begin{aligned} u(t) &= y_{11} + \int_{\tau}^t r(s)L_0(r_1(s), e^{\lambda(\mu)(s-\tau)}u(s), \mu)u(s)ds \\ &\quad + \int_{\tau}^t e^{-\lambda(\mu)(s-\tau)}r_1(s)\epsilon_1(s)L_1(r_1(s), \epsilon_1(s), e^{-\lambda(\mu)(s-\tau)}u(s), \mu)ds. \end{aligned} \quad (67)$$

Here

$$r_1(t) = e^{-\frac{1}{2}t}r_{10}, \quad \epsilon_1(t) = e^{(t-\tau)}\epsilon_{11}.$$

Now we consider the closed subset $\Gamma(\delta)$ of the Banach space $C([0, \tau]; \mathbb{R})$, equipped with the $\sup_{t \in [0, \tau]}$ -norm, with $u(t) \leq \delta$ and $u(\tau) = y_{11} \leq \frac{\delta}{2}$.

We then proceed as in [12] and let $\Theta(u)(t)$ denote the right hand side of (67). We then show that Θ is a contraction on Γ , upon choosing the constants appropriately. For this, let $\bar{L}_0(t, u, \mu) = L_0(r(t), e^{\lambda(\mu)(t-\tau)}u, \mu)$, $\bar{L}_1(t, u) = L_1(r_1(t), \epsilon_1(t), e^{-\lambda(\mu)(t-\tau)}u, \mu)$. Then for any $k \in \mathbb{N}$ it is straightforward to show that there is a $C(k) > 0$ so that

$$|D^i \bar{L}_0(t, u, \mu)|, |D^i \bar{L}_1(t, u, \mu)| \leq C(k),$$

for all $t \in [0, \tau]$, $|u| \leq \delta$. where D^i , $i = (i_1, i_2)$ denotes the partial derivative of order $0 \leq i_1 + i_2 \leq k$ with respect to u and μ . Notice, in particular that upon differentiating L_0 and L_1 with respect to u , we obtain terms having factors of the form

$$(\tau - t)^{i_1} e^{\lambda(\mu)(t-\tau)}.$$

Such terms are clearly bounded by a constant $c(i_1) > 0$ for each i_1 for $t \in [0, \tau]$; in fact, we may take $c(i_1) = c(k)$ for all $0 \leq i_1 \leq k$ where

$$c(k) = \left(\frac{k}{\lambda}\right)^k e^{-k} \geq u^k e^{-\lambda u} \quad \text{for all } u \geq 0. \quad (68)$$

All other factors and terms can be bounded in a similar way.

We then have the following: If $u \in \Gamma(\delta)$, then $\Theta(u)(\tau) = y_{11}$ and

$$|\Theta(u)(t)| \leq \frac{\delta}{2} + (4r_{10}\delta + \frac{e^{-1}}{1-\lambda}r_{10}\epsilon_{11})C(k). \quad (69)$$

Here we have used that

$$\int_t^{\tau} e^{-s} ds \leq 4, \quad \int_t^{\tau} e^{-\lambda(\mu)(s-\tau)}r_1(s)\epsilon_1(s)ds \leq \frac{e^{-1}}{1-\lambda}.$$

The last inequality follows from $\frac{1}{\alpha}(e^{\alpha x} - 1) \leq xe^{\alpha x}$ for all $\alpha \neq 0$, $x \geq 0$ and (68).

Consequently, we take ϵ_{11}, r_{10} and μ so small that

$$(4r_{10}\delta + \frac{e^{-1}}{1-\lambda(\mu)}r_{10}\epsilon_{11})C(k) < \frac{\delta}{2}.$$

Then $\Theta : \Gamma(\delta) \rightarrow \Gamma(\delta)$. Moreover, if $u, \tilde{u} \in \Gamma(\delta)$ then

$$|\Gamma(u)(t) - \Gamma(\tilde{u})(t)| \leq 2(4r_{10}\delta + \frac{e^{-1}}{1-\lambda}r_{10}\epsilon_{11})C(k)\|u - \tilde{u}\| \leq \delta\|u - \tilde{u}\|.$$

Consequently for all $\delta > 0$ small enough $\Theta : \Gamma(\delta) \rightarrow \Gamma(\delta)$ is contraction; we denote the unique fixed-point – existence of which follows from Banach’s fixed point theorem – by $\underline{u}(t, \tau, \epsilon_{11}, r_{10}, y_{11}, \mu)$. From (69) we find the estimate

$$|\underline{u}(t, \tau, \epsilon_{11}, r_{10}, y_{11}, \mu)| \leq y_{11} + \frac{\delta}{2}.$$

Writing $\underline{u} = y_{11} + \phi$ we obtain the desired form Proposition 3.3. Regarding the statements on the partial derivatives of ϕ , including those with respect to y_{11}, μ that are $\mathcal{O}(\delta)$, we can proceed completely analogously by setting up fixed-point equations for such partial derivatives. We leave out further details, see [12].